

Technical University of Denmark



## Physics Department. Annual progress report 1 January - 31 December 1974

Forskningscenter Risø, Roskilde

*Publication date:*  
1974

*Document Version*  
Publisher's PDF, also known as Version of record

[Link back to DTU Orbit](#)

*Citation (APA):*  
Research Establishment Risø, R. (1974). Physics Department. Annual progress report 1 January - 31 December 1974. (Denmark. Forskningscenter Risoe. Risoe-R; No. 320).

## DTU Library

Technical Information Center of Denmark

---

### General rights

Copyright and moral rights for the publications made accessible in the public portal are retained by the authors and/or other copyright owners and it is a condition of accessing publications that users recognise and abide by the legal requirements associated with these rights.

- Users may download and print one copy of any publication from the public portal for the purpose of private study or research.
- You may not further distribute the material or use it for any profit-making activity or commercial gain
- You may freely distribute the URL identifying the publication in the public portal

If you believe that this document breaches copyright please contact us providing details, and we will remove access to the work immediately and investigate your claim.

Danish Atomic Energy Commission  
Research Establishment Risø

---

Physics Department  
Annual Progress Report

1 January – 31 December 1974

December 1974

*Sales distributors:* Jul. Gjellerup, 87, Sølvgade, DK-1307 Copenhagen K, Denmark

*Available on exchange from:* Library, Danish Atomic Energy Commission, Risø, DK-4000 Roskilde, Denmark



December 1974

Risø Report No. 320

Danish Atomic Energy Commission

Research Establishment Risø

PHYSICS DEPARTMENT

ANNUAL PROGRESS REPORT

1 January - 31 December 1974

edited by

H. Bjerrum Møller and B. Lebech

This report contains unpublished results and should not be  
quoted without permission from the authors.

# CONTENTS

	Page
Summary .....	7
1. Solid State Physics (Neutron Scattering) .....	12
Spin Waves in Tb. I: Two-Ion Magnetic Anisotropy ...	12
Spin Waves in Tb. II: Magnon-Phonon Interaction .....	13
Spin Waves in Tb. III: Magnetic Anisotropy at Zero Wave Vector .....	13
Molecular-Field Calculation of the Magnetic Structure of Er .....	14
Calculations of Spectra in Solids .....	15
Theoretical Calculation of the Exchange Interaction in Gd .....	15
Calculation of the Magnetization in Tb and Dy .....	16
Neutron Diffraction Studies of Tb-Tm Alloys .....	17
Spin Wave Analysis of Specific Heat and Magnetization in EuO and EuS .....	17
Magnetic Ordering of Single Crystal Pr .....	19
Magnetization and Transition Temperatures of Pr-Nd Alloys .....	20
Theory for the Critical Temperature of Systems with Two-Order Parameters .....	22
Magnetic Excitations in Pr Metal .....	23
Theory of Magnetic Excitations in Pr .....	27
Coupling between the Magnetic Excitations and the Phonons in Pr .....	28
Magnetic Form Factor of Pr-26% Nd .....	29
Crystal Fields in Er-98% Y Studied by Neutron Scattering .....	31
Crystal Field Parameters and Phase Transitions in ErSb .....	31
Crystal Field Splitting in NdN .....	32
Crystal Fields in Rare Earth Al <sub>2</sub> Compounds .....	33
Crystal Field Theory Including Fluctuations in the Molecular Field .....	33
The Dipolar Coupled Ising Ferromagnet LiTbF <sub>4</sub> .....	34
Nuclear and Electronic Antiferromagnetism in HoPO <sub>4</sub> .....	35

	Page
Magnetic Properties of $\text{MnNb}_2\text{O}_6$ .....	36
Spin Wave Dispersion and Sublattice	
Magnetization in $\text{NiCl}_2$ .....	37
Excitations in a Two-Dimensional Random Anti-ferromagnet .....	37
Canonical Bands of Metals .....	38
Potential Parameters of Metals .....	39
Crystal Structures of Transition Metals .....	40
Electronic Structure of hcp Transition Metals .....	40
Lattice Dynamics of $\text{Cu}_2\text{O}$ .....	41
Phonons in $\text{C}_{10}\text{D}_8$ .....	43
The Phase Transition in $\text{C}_{10}\text{F}_8$ .....	43
Neutron Scattering in $\text{C}_2\text{F}_6$ .....	45
The Structural Phase Transition	
in Solid DCN .....	46
Hydrogen Adsorbed on Graphite .....	47
Neutron Scattering in Solid $\text{H}_2$ under	
Moderately High Pressure .....	49
Neutron Scattering in Liquid $\text{H}_2$ .....	51
Neutron Scattering in Liquid $\text{N}_2$ .....	52
The Solid-Liquid Phase Transition .....	53
Hydrodynamic Fluctuations near the Convection	
Instability in the Nematic Liquid Crystal PAA .....	54
Neutron Diffraction Study of Amorphous	
Solid Water .....	55
Inelastic Paramagnetic Neutron Scattering	
in Ce Metal under Pressure .....	55
Pressure-Induced Phase Transition in $\text{TeO}_2$ .....	56
Pressure Dependence of the Néel Temperature	
of Cr Single Crystal .....	57
Neutron Scattering from Crystalline Se .....	58
Determination of the Debye-Waller Factor of	
$\text{MgO}$ Powder by Elastic Neutron Scattering .....	58
Neutron Slowing-Down by Bragg Reflection	
from a Moving Crystal .....	60

	Page
2. Plasma Physics .....	61
Solid H <sub>2</sub> Film .....	61
Pellet-Refuelling Problem.	
I: Theoretical Aspects .....	63
II: Acceleration .....	64
Rotating Plasma Measurements.	
I: Charge Exchange Neutrals .....	64
II: Doppler Broadening .....	65
III: Electron Temperature .....	65
Pellet-Rotating Plasma Interaction.	
I: Pellet Velocity Measurements .....	65
II: Spectroscopy .....	66
Investigation of the Farley Instability	
in the Q-Machine .....	66
Kelvin Helmholtz Instability .....	67
Electron Heating at the Cyclotron Resonance .....	68
Ion Beam Instability .....	68
3. Nuclear Physics .....	69
An Attempt to Form the <sup>236</sup> U Fission Isomer	
with Thermal Neutrons .....	69
4. Meteorology .....	70
Change of Terrain Roughness .....	70
Atmospheric Gravity Waves .....	71
Simulation of Atmospheric Turbulence .....	73
Time Series Analysis .....	73
Digital Noise .....	74
Air-Sea Interaction .....	76
Fine Structure Experiment .....	76
Climatology in Greenland .....	78
Numerical Modelling of the Planetary	
Boundary Layer .....	80
Stress-Profile Experiment .....	81
Wind Power .....	82
Dynamic Wind Loading .....	83



	Page
Applied Meteorology.	
I: Site Evaluation .....	84
II: Air Pollution .....	85
Air Pollution Statistics .....	86
5. Liquid N <sub>2</sub> and He Plant .....	87
6. Educational Activities and Publications .....	88
7. Staff of the Physics Department .....	103
8. Visiting Scientists .....	107

## SUMMARY

The research work in the Physics Department at Risø covers four main fields:

Solid-State Physics (Neutron Scattering)

Plasma Physics

Nuclear Spectroscopy

Meteorology

The principal activities in these fields are presented in this report covering the period from 1 January to 31 December 1974.

The solid-state physics section utilizes thermal neutron beams from the DR 3 reactor for experimental studies of solids and liquids. Six neutron spectrometers are available for these experiments: five are triple-axis and one is a double-axis instrument. An additional diffractometer is used for structural studies by the Institute of Chemistry, University of Århus. A liquid-hydrogen cold source is being installed in the DR 3 reactor. Cold neutrons will presumably be available from the summer of 1975. The construction of neutron-conducting tubes from the cold source to an experimental hall was continued. The tubes are planned to be installed in the fall of 1975.

Scientific investigations can be roughly grouped in the following fields: magnetism, lattice dynamics, liquids, and amorphous materials.

As in previous years, most of the work on magnetism was concerned with rare earth metals, the emphasis shifting from the heavy to the light rare earth metals.

Several years of experiments on spin waves in the heavy rare earth metal Tb have now been analysed, and a complete report on the results was issued. Neutron diffraction studies on heavy rare earth alloys (Tb-Tm) were initiated. Theoretical calculations were made of the exchange interaction in Gd, of the magnetic structure of Er, and of the magnetization of Tb and Dy in high magnetic fields.

Among the light rare earth metals, most interest has concentrated on Pr, and in particular on the possibility of magnetic ordering at low temperatures. Neutron diffraction on single crystals showed no evidence of magnetic ordering down to 0.4 K, but diffraction measurements on alloys (Pr-Nd), as well as measurements of the exciton dispersion relation, show that Pr is very close to spontaneous order. A strong coupling between the magnetic excitons and phonons was observed in a magnetic field. Theoretical calculations for Pr and the alloys agree well with the experimental results.

A number of rare earth alloys (Er-Y, ErSb, NdN,  $\text{REAl}_2$ ) with large crystal field anisotropy (relative to the exchange interaction) were investigated and the crystal field parameters determined. The critical scattering was investigated in a dipolar-coupled Ising ferromagnet ( $\text{LiTbF}_4$ ) and the nuclear spin ordering of Ho in  $\text{HoPO}_4$  was observed in the neutron diffraction pattern at low temperatures.

The magnetic properties of a number of compounds containing transition elements ( $\text{MnNb}_2\text{O}_6$ ,  $\text{NiCl}_2$ ,  $\text{Rb}_2\text{Mn}_{0.5}\text{Ni}_{0.5}\text{F}_4$ ) were investigated by elastic and inelastic neutron scattering. For  $\text{Rb}_2\text{Mn}_{0.5}\text{Ni}_{0.5}\text{F}_4$  it was found that a simple random alloy model predicts the measured dispersion relations.

The canonical bands and the potential parameters which describe the electronic energy bands of metals were determined for a number of structures and metals. The method was applied to the hop transition metals.

The lattice dynamics of several molecular crystals ( $\text{Cu}_2\text{O}$ ,  $\text{C}_{10}\text{D}_8$ ,  $\text{C}_{10}\text{F}_8$ ,  $\text{C}_2\text{F}_6$ , DCN,  $\text{H}_2$ ) were investigated. In the plastic phase of  $\text{C}_2\text{F}_6$  no phonons were seen, but a wave-vector-dependent, quasi-elastic mode was observed. In DCN the observation of a transverse phonon mode of extremely low energy, near the structural phase transition at  $T_c = 160$  K, suggests that the transition is driven by a soft mode. The previous, detailed investigations of phonons in the quantum solid,  $\text{H}_2$ , were supplemented by measurements under pressure (0-2 kbar) and by a study of a monolayer of  $\text{H}_2$  adsorbed on grafoil.

The previous scattering measurements on liquid  $H_2$  and  $N_2$  were analysed further. In order to verify a dislocation theory for melting, the solid-liquid phase transition was investigated by studying the phonons in Pb and Al near melting. The hydrodynamic instability at the convection threshold was studied in the nematic phase of the liquid crystal PAA.

The high pressure equipment, described in last year's progress report, was used in several experiments. Among these were studies of the pressure-induced phase transition in  $TeO_2$  and the pressure dependence of the Néel temperature in Cr.

The plasma physics section works under a contract of association between the Danish Atomic Energy Commission and Euratom. The activities are centered on technology of interest for future fusion reactors (utilizing a puffatron) and on basic plasma physics (utilizing a Q-machine).

The puffatron produces a hot rotating plasma in a strong radial electric and axial magnetic field. Studies of the interaction between the plasma and solid hydrogen pellets were pursued both experimentally and theoretically, with a possible refuelling scheme for future fusion reactors in mind. This scheme requires an acceleration technique which is able to accelerate small pellets to a velocity of the order of  $10^3$ - $10^4$  m/s. The necessary velocity depends on the ablation rate of a pellet inside a fusion plasma. The activities were subdivided into the following areas: (a) investigation and development of acceleration techniques, (b) measurements of parameters which characterize the plasma used to study the interaction between pellet and plasma, and (c) a study of the interaction itself.

The Q-machine produces a relatively cold dc-plasma (2000 K) of ionized Cs. A number of instabilities in this plasma were investigated. The magnetic field was modified into a cusp field and the Farley instability was studied in a case where a radial electric field was applied to the plasma. An experiment to simulate the Kelvin Helmholtz instability was also set up in the Q-machine but no instability was observed.

The electron temperature in the Q-machine was increased by a factor of ten. To achieve this, microwave energy was fed into the plasma via a microwave horn or via a microwave cavity resonator. The electron heating occurs when the microwave frequency resonates with the electron cyclotron frequency.

The nuclear physics section works on problems related to fission. A search for the formation of fission isomers in  $^{235}\text{U} + n$  is being finished. No significant indication of isomers was found in spite of the increased sensitivity of the experimental method as compared to earlier measurements.

The meteorology section is primarily engaged in studies of the planetary boundary layer. The efforts can be roughly classified as follows: (1) micrometeorological research, (2) climatological investigations, (3) development of meteorological instruments, and (4) applied meteorology.

The micrometeorological research aims at descriptions of the structure of atmospheric turbulence and its dependence on external parameters such as surface characteristics and the synoptic weather situation. An important goal is parameterization of the transport properties of atmospheric turbulence, so that the planetary boundary layer can be realistically incorporated in numerical weather prediction schemes.

Air-sea interaction is a problem to which the section pays increasing attention. The interest is primarily concentrated on turbulence and fluxes in the lowest 20 m above the sea. The section continues its participation in the Joint North Sea Wave Project (JONSWAP-75) and in Project Kattegat-75.

At Esbo a 120 m tower is available for experimental work. Meteorological parameters such as wind speed and direction, temperature and humidity are measured routinely at a number of heights. As a result of the measurements, data records are available containing 16 years of hourly readings. The records are used extensively by the section and by others.

For field experiments the section has at its disposal a 50 m mobile tower and a data acquisition system installed in a van. The digital data system is capable of sampling 60 signals simultaneously at a rate of 200 times per second.

An experimental study is in progress of the influence of abrupt changes in surface roughness on the flow immediately above the surface. Three instrumented towers have been put up along a line running inland at a right angle to the north shore of the Risø peninsula. In the summer of 1974 a comprehensive experiment was carried out at Risø concerning the small-scale, high-frequency behaviour of atmospheric turbulence. Visiting scientists from the U.S.A. and Canada took part in the experiment.

The effect of excitation of internal gravity waves on the development of an unstable boundary layer capped by an inversion was investigated theoretically. A high-resolution model of the planetary boundary layer suitable for use with mesoscale dynamic models was developed in cooperation with the Department of Meteorology at Pennsylvania State University. The analysis of climatological data from Greenland, Risø, and other locations in Denmark was continued. Special emphasis is given to analyses in terms of spectral characteristics of weather and climate fluctuations. The meteorology section now operates ten automatic meteorological observatories of which three in North Greenland are operated jointly with the Danish Meteorological Institute.

This year as earlier the meteorology section undertook a number of tasks of an applied nature. Among them were: site evaluation for nuclear power stations and dispersion modelling, air pollution studies, evaluation of dynamic effects of wind on engineering structures, development and testing of meteorological instruments, and evaluation of wind power as an alternative energy source.

## 1. SOLID STATE PHYSICS (NEUTRON SCATTERING)

### Spin Waves in Tb. I: Two-Ion Magnetic Anisotropy

(J. Jensen, J.G. Houmann, and H. Bjerrum Møller)

The energies of spin waves propagating in the c-direction of Tb have been studied by inelastic neutron scattering, as a function of a magnetic field applied along the easy and hard directions in the basal plane, and as a function of temperature. From a general spin Hamiltonian, consistent with the symmetry, we can deduce the dispersion relation for the spin waves in a basal plane ferromagnet. This phenomenological spin wave theory accounts for the observed behaviour of the magnon energies in Tb.

The two  $\vec{q}$ -dependent Bogoliubov components of the magnon energies are derived from the experimental results, which are corrected for the effect of the direct coupling between the magnons and the phonons, and for the field dependence of the relative magnetization at finite temperatures. A large  $\vec{q}$ -dependent difference between the two energy components is observed, showing that the anisotropy of the two-ion coupling between the magnetic moments in Tb is substantial. The  $\vec{q}$ -dependent anisotropy deduced at 4.2 K is of the same order of magnitude as the isotropic part, and depends strongly on the orientation of the moments in the basal plane. The rapid decrease of both the axial and the basal plane anisotropy with increasing temperatures implies that the two-ion coupling is effectively isotropic above 150 K.

We can present arguments for concluding that, among the mechanisms which may introduce anisotropic two-ion couplings in the rare-earth metals, the modification of the indirect exchange interaction by the spin-orbit coupling of the conduction electrons is of greatest importance.

### Spin Waves in Tb. II: Magnon-Phonon Interaction

(J. Jensen and J.G. Houmann)

The selection rules for the linear couplings between magnons and phonons propagating in the c-direction of a simple basal plane hcp-ferromagnet may be determined by general symmetry considerations. The acoustic-optical magnon-phonon interactions observed in the heavy rare-earth metals have been explained by Liu<sup>1)</sup> as originating from the mixing of the spin states of the conduction electrons due to the spin-orbit coupling. We find that this coupling mechanism introduces interactions which violate the selection rules for a simple ferromagnet.

The interaction between the magnons and phonons propagating in the c-direction of Tb has been studied experimentally by means of inelastic neutron scattering. The magnons are coupled to both the acoustic and optical transverse phonons. By studying the behaviour of the acoustic-optical coupling we can conclude that it is a spin-mixed induced coupling as proposed by Liu. The coupled magnon-transverse phonon system for the c-direction of Tb has been analysed in detail, and the strengths of the couplings deduced as a function of wave vector combining the experimental studies with the theory.

### Spin Waves in Tb. III: Magnetic Anisotropy at Zero Wave Vector

(J.G. Houmann, J. Jensen, and P. Touborg (Technical University of Denmark))

The energy gap at zero wave vector in the spin wave dispersion relation of ferromagnetic Tb has been studied by inelastic neutron scattering. The energy was measured as a function of temperature and applied magnetic field, and the dynamic anisotropy parameters were deduced from the results. The axial anisotropy is found to depend sensitively on the orientation of the magnetic moments in the basal plane. This behaviour can be

---

<sup>1)</sup> S.H. Liu, Phys. Rev. Lett. 29, 793 (1972).



shown to be a convincing indication of considerable two-ion contributions to the magnetic anisotropy at zero wave vector. With the exception of the six-fold basal plane anisotropy of the unstrained lattice, the dynamic anisotropy parameters deduced from our results agree with macroscopic measurements both with respect to the magnitudes (at zero temperature) and the temperature dependences. The deviations observed cannot be explained by existing theories that include the effects of zero point deviations from the fully aligned ground state, and we tentatively propose polarization-dependent two-ion couplings as their origin.

#### Molecular Field Calculation of the Magnetic Structure in Er (J. Jensen)

Neutron diffraction studies of the magnetic structure of  $\text{Er}^{2+}$  have revealed the existence of three distinct regions of long-range magnetic order:

- (1) For  $84 \text{ K} > T > 52 \text{ K}$ : The c-axis moments are ordered in a sinusoidal structure, with a period of 7-8 atomic layers and with the modulation vector parallel to the c-axis.
- (2) For  $52 \text{ K} > T > 20 \text{ K}$ : A spiral ordering of the basal plane components of the moment superimposed on the c-axis sinusoidal structure.
- (3) For  $T < 20 \text{ K}$ : A c-axis cone structure.

We have attempted to reproduce these magnetic structures in Er within a molecular-field approximation. The two-ion coupling is considered to be described by the inter-planar exchange parameters determined from the dispersion of the spin waves in the conical phase<sup>3)</sup> (the deduced two-ion anisotropy is also included). The crystal field parameters of Er diluted in Y have been determined by Høg and Touborg<sup>4)</sup>. By a slight modification of  $B_{20}$ , and a somewhat larger change of the other three crystal field parameters, we have been able to obtain a reasonable fit to the

---

<sup>2)</sup> M. Habenschuss, C. Stassis, S.K. Sinha, H.W. Deckmann, and F.H. Spedding, Phys. Rev. B 10, 1020 (1974) and M. Atoji, to be published.

<sup>3)</sup> J. Jensen, J. Phys. F 4, 1065 (1964).

<sup>4)</sup> J. Høg and P. Touborg, Phys. Rev. B 9, 2920 (1974).

magnetization data at 4.2 K, and to reproduce the phases (1) and (3) whereas the present choice of parameters fails to predict the phase (2). A difference, between the parameters determined by Høg and Touborg, for dilute Er and those describing pure Er is very likely to occur because of the presence of strong two-ion anisotropy in pure Er<sup>3</sup>). It is not possible to separate the intraplanar two-ion contributions from the single-ion parameters. The model calculations are being continued in an attempt to improve the agreement with the experimental results.

### Calculations of Spectra in Solids

(P.-A. Lindgård)

The real and imaginary parts of the conduction electron response function were calculated numerically and discussed using the linearized integral method. A frequency expansion for the real part around a characteristic frequency, which considerably simplifies the expressions to be calculated, has been suggested. The static susceptibilities for Gd, Tb and Dy have been calculated using the relativistic APW energy bands<sup>5)</sup>. The results for Gd are significantly different from those calculated by Liu et al.<sup>6)</sup> using the root sampling method.

### Theoretical Calculation of the Exchange Interaction in Gd

(P.-A. Lindgård and B.N. Harmon (Iowa State University, U.S.A.))

The indirect (RKKY) exchange matrix elements  $j(\vec{k}, \vec{k}')$  between the conduction electrons and the local 4f-moments have been calculated for Gd using non-relativistic APW wave functions and assuming an unscreened Coulomb interaction. The matrix elements exhibit a great deal of structure as a function of  $\vec{k}$  and  $\vec{k}'$  and are largest for d-like conduction electrons. The structure is associated with the change in symmetry of the wave functions as a function of wave vector. at  $\vec{k} \sim \vec{k}'$  the wave functions have the same symmetry

<sup>5)</sup> S.C. Keeton and T.L. Loucks, *Phys. Rev.* **188**, 672 (1968).

<sup>6)</sup> S.H. Liu, R.P. Gupta, and S.K. Sinha, *Phys. Rev.* **B 4**, 1100 (1971).

and  $j(\vec{k}, \vec{k}')$  is large. At  $\vec{k}-\vec{k}'$  large, the wave functions are with high probability orthogonal and  $j(\vec{k}, \vec{k}')$  is therefore small.

The matrix elements and energy eigenvalues are used to calculate the magnon spectrum of Gd along the  $\Gamma$ -A symmetry direction. The calculation demonstrates: (1) the need to include the  $\vec{k}$  and  $\vec{k}'$  dependence of the matrix elements, and (2) the importance of including transitions from all bands below the Fermi energy to bands well above. The dispersion relations are found to be rather insensitive to fine details in the band structure. Comparison of the theoretical results with the magnitude of the conduction electron polarization and the magnon spectrum indicates that agreement is obtained if the matrix elements are reduced by a constant scale factor of about two. This reduction may be caused by screening effects. These are not taken into account in our calculations. In view of this being a first principle calculation the agreement is surprisingly good.

#### Calculation of the Magnetization in Tb and Dy

(P.-A. Lindgård and G.J. Cock (University of Amsterdam, The Netherlands))

The spin wave theory by Lindgård and Danielsen<sup>7)</sup> was used to analyse the magnetization data of Tb and Dy in high magnetic fields (0-40 T), applied in the easy and hard directions, at  $T = 1.8, 4.2$ , and  $77$  K. The experimental spin wave dispersion relations were parametrized by real space exchange constants and used in the Brillouin sum which is involved in the calculation of the spin wave population. A reasonable agreement between theory and experiment was obtained using the known<sup>8)</sup> anisotropy and magnetoelastic parameters.

---

<sup>7)</sup> P.-A. Lindgård and O. Danielsen, Phys. Rev. B, Dec. (1974),

<sup>8)</sup> A.R. Mackintosh and H. Bjerrum Møller, Magnetic Properties of Rare Earth Metals, (R.J. Elliot, Editor), Plenum Press, London (1972).

## Neutron Diffraction Studies of Tb-Tm Alloys

(P.Aa. Hansen)

Neutron diffraction measurements, especially by Koehler et al.<sup>9)</sup>, on alloys of heavy rare earths have shown that the magnetic structures of these alloys are similar to those observed in the pure elements. These experiments may all be interpreted, if one assumes that the magnetic moments of the constituents of the alloy are fully aligned, although the experimental error is quite large.

The magnetic moment of Tb is constrained to the basal plane by large anisotropy forces and Tm has a large axial anisotropy which constrains the moments to lie along the c-axis. The Tb-Tm alloy system thus seems ideally suited for experimental determination of whether single-ion or two-ion anisotropy is important in the heavy rare earths.

A preliminary experiment has been done on a single crystal Tb-12% Tm alloy. Within the experimental accuracy the Tb and Tm moments lie in the basal plane. This is to be expected, because the exchange field from the Tb ions is large compared to the anisotropy forces acting on the Tm ions. On the other hand one would not expect the field from the Tm ions to be strong enough to lift the Tb moments out of the basal plane. The Tm rich end of the systems is therefore more interesting in this connection. Measurements on single crystals of these alloys (Tb-50% Tm, and Tb-90% Tm) will be made in the near future.

## Spin Wave Analysis of Specific Heat and Magnetization in EuO and EuS

(O.W. Dietrich, A.J. Henderson, Jr.<sup>\*</sup>, and H. Meyer<sup>\*</sup> (<sup>\*</sup>Duke University, Durham, U.S.A.))

Previously published results on the exchange constants in EuO and EuS determined by the methods of specific heat, NMR and neutron scattering do not agree. We have reanalysed the specific heat and

<sup>9)</sup> A.H. Millhouse and W.C. Koehler, Intern. J. Magnetism 2, 389 (1971).

NMR measurements using a detailed treatment of the dipolar effects and Brillouin zone summation. The new analysis shows that the various measurements agree within acceptable limits. It is in particular confirmed that the next nearest neighbour coupling in EuO is ferromagnetic, a result which has been anticipated by theoretical conjecture.

#### Magnetic Ordering of dhcp Single Crystal Pr

(B. Lebech, J.G. Houmann, and M. Chapellier)

The elastic scattering from a large (670 mm<sup>3</sup>) Pr single crystal was studied at 0.4, 1.8, and 4.2 K using triple-axis neutron spectrometry. The crystal was mounted in a pumped <sup>3</sup>He cryostat with a <110>-direction vertical and perpendicular to the scattering plane. Systematic scans at two different incident energies (14.2 meV and 5.1 meV) were made around the (001) and (003) reciprocal lattice points. The scan direction was parallel to the (100)-direction,  $\Gamma M$ , since the exciton dispersion relation<sup>10)</sup> shows an absolute minimum at  $q \sim 0.25 \text{ \AA}^{-1}$  along this direction. We did not observe any difference between the elastic scattering at 4.2, 1.8, and 0.4 K. However, we did observe additional scattering centered symmetrically around (003) at (Q03) and ( $\bar{Q}$ 03) ( $Q \sim 0.125$  times the (100) reciprocal lattice vector) at all three temperatures (fig. 1). The overall linewidth of this scattering is about 5.5 times the full width at half maximum of the nuclear (100) Bragg reflection and the peak-intensity 2000 times smaller than the peak-intensity of the (100) reflection. Similar, but less intense elastic scattering was observed around (001). Because the scattering is temperature independent we may conclude that there is no evidence of magnetic ordering in single crystal Pr down to 0.4 K.

---

<sup>10)</sup> J.G. Houmann, M. Chapellier, A.R. Mackintosh, P. Bak, O.L. McMasters, and K.A. Gschneidner, Jr., to be published in Phys. Rev. Lett. (1975).

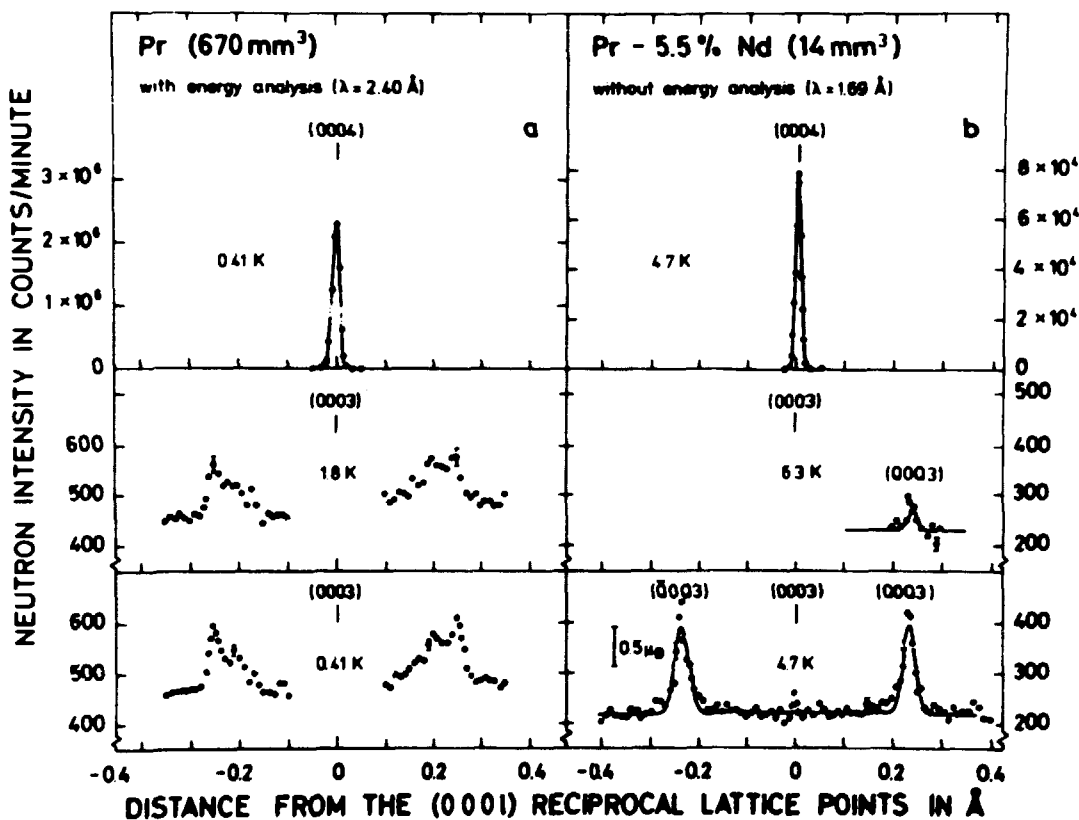


Fig. 1. Neutron diffraction scans parallel to the  $\langle 100 \rangle$ -direction through the (003) and (004) reciprocal lattice points for Pr (a) and Pr-5.5% Nd (b). The elastic scattering observed around (003) in Pr is temperature independent.

# Magnetization and Transition Temperatures of Pr-Nd Alloys

(B. Lebech, K.A. McEwen (University of Salford, U.K.),  
and P.-A. Lindgård)

Single crystals of Pr-Nd alloys with Nd concentrations of 3.0%, 5.5%, 26.3%, and 100% have been studied by neutron scattering. These alloys order magnetically at low temperature in a modulated antiferromagnetic structure characterized by a modulation

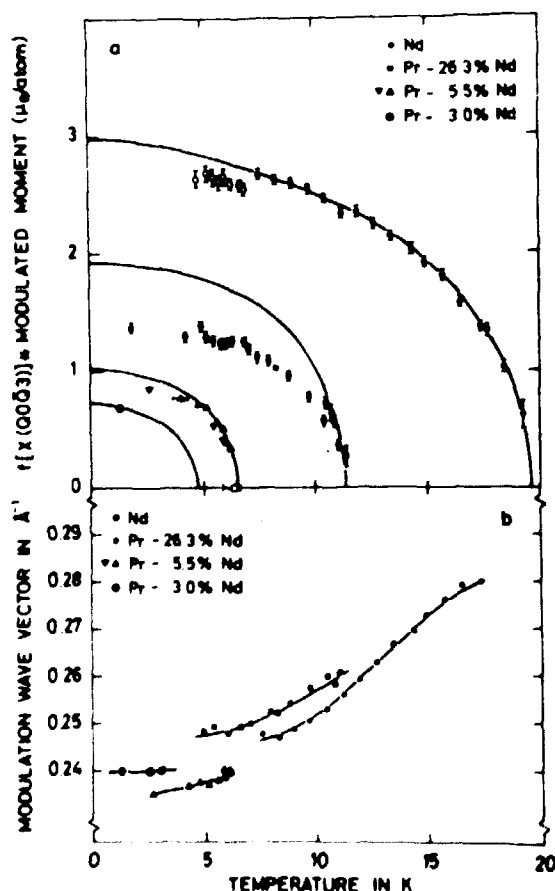


Fig. 2. Temperature dependence of the modulated moment at the hexagonal sites in Pr-Nd alloys derived from the intensities of the  $(\bar{Q},0,3)$  magnetic satellites. The experimental results are compared to the calculated temperature dependence of the total ordered moments (solid lines) in the alloys in a molecular field theory. Below 7.8 K the moments on the cubic sites in Nd are ordered, and below  $\sim 6$  K an additional ferromagnetic component of the moment is observed in Pr-26.3% Nd.

vector,  $\vec{Q}$ , in a  $\langle 100 \rangle$  direction. The temperature and magnetic field dependence of the magnetization have been measured as a function of the concentration. These results have been analysed on the basis of a molecular field theory<sup>11)</sup> for alloys of atoms with different crystal field level schemes. Assuming long range exchange interaction, which is valid for the rare earths, the theory can be applied to all concentrations. Using the crystal field parameters for Pr determined by Rainford<sup>12)</sup> we find:

- (1) The crystalline electric field acting on Nd is  $\sim 2.5$  times smaller than that acting on Pr.
- (2) The ratio between the exchange and crystal field energy for Pr is  $0.95 < 1$ , which shows that Pr is near the critical ratio for ordering.

Since Pr is so close to criticality only a small amount of impurity may be sufficient to give magnetic order. Thus if a 99.9% pure Pr crystal is solely contaminated by Nd, it would order at 0.4 K.

In fig. 2 we compare the calculated temperature dependence of the total ordered moments in the alloys (solid lines) to the temperature dependence of the amplitude of the antiferromagnetic moment determined by neutron diffraction. The exchange parameters at wave vector  $Q$  are derived from best fits to the experimental data and found to be

$$J_{\text{Pr-Pr}}(Q) = 0.67 \text{ K}, J_{\text{Nd-Nd}}(Q) = 1.08 \text{ K}, \text{ and } J_{\text{Pr-Nd}}(Q) = 0.86 \text{ K}.$$

At low temperatures a ferromagnetic component of the moment develops ( $\sim 0.8\mu_B$  at 1.2 K) in the 26.3% alloy, which may account for the discrepancy between the observed and the calculated moment in this alloy.

---

<sup>11)</sup> P.-A. Lindgård, p. 22.

<sup>12)</sup> B.D. Rainford, **Magnetism and Magnetic Materials AIP Conference Proceedings** 5, 591 (1972).



# Theory for the Critical Temperature of Systems with Two Order Parameters

(P.-A. Lindgård)

A simple molecular field theory is developed for alloys of atoms with different crystal field splittings. If both constituents are singlet ground state atoms, interesting mixture curves occur for  $T_c$  versus concentration. Some examples are shown in fig. 3.

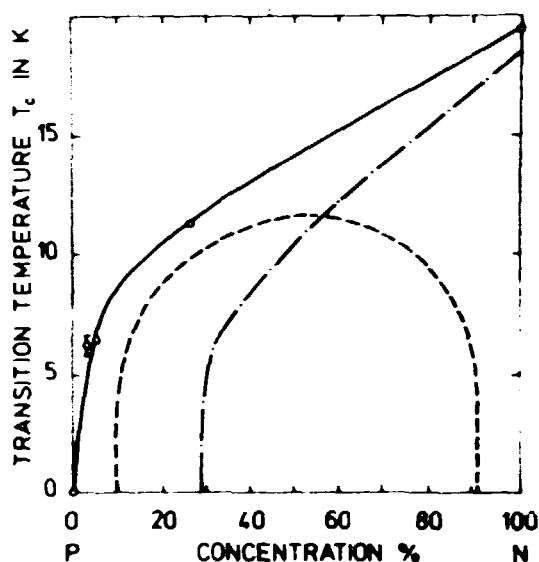


Fig. 3. The transition temperatures versus concentration for alloys of crystal field split systems. The full curve shows a (singlet-doublet)-(Kramers' doublet) system, for instance  $P = \text{Pr}$  and  $N = \text{Nd}$ . The critical ratio for Pr is found to be  $0.95 < 1$ . The dot-dashed curve shows the typical behaviour of an alloy of two (singlet-doublet) systems, as for instance  $P = \text{Pr}$  and  $N = \text{Tb}$ , for which P is under-critical and N is over-critical. The dashed curve is typical of a mixture of two strongly interacting, under-critical systems. The points show the Néel temperatures for Pr-Nd alloys obtained by neutron diffraction<sup>13)</sup>.

<sup>13)</sup> P. Indrich, F.A. McEwen, and P.-A. Lindgård, p. 20.

For the determination of  $T_c$  it is sufficient to consider simplified level schemes. To obtain the magnetization versus temperature the full level scheme is necessary. For the Pr-Nd alloy a (singlet-doublet)-(Kramers' doublet) model gives excellent agreement between  $T_c$  observed experimentally and that calculated from this theory. Since Nd has a Kramers' doublet ground state even an infinitely small concentration can give rise to order (in the molecular field theory). Because of the strong planar anisotropy Pr-Tb alloy would be an alloy of two (singlet-doublet) systems. Such an alloy would order only at a finite Tb concentration. Since Tb gives rise to a strong exchange interaction it is also possible to study the  $\text{Pr}^{3+}$  ion in "magnetic" molecular fields up to 100 T.

The theory is applicable to a much wider range of phenomena: that is mixtures of systems with a different response function to a conjugated field. The order parameters may for example be magnetic moments or quadrupole moments.

#### Magnetic Excitons in Pr Metal

(J.G. Houmann, M. Chapellier, A.R. Mackintosh, B.D. Rainford (Imperial College, London), O.D. McMasters<sup>\*</sup>, and K.A. Gschneidner, Jr.<sup>\*</sup> (<sup>\*</sup>Iowa State University, U.S.A.))

For a number of years there has been controversy about the existence of magnetic ordering in Pr. An antiferromagnetic structure below a Néel temperature of 25 K was observed by neutron diffraction on a polycrystalline sample by Cable et al.<sup>14)</sup>. However, neutron diffraction studies on single crystals have failed to show any evidence of antiferromagnetism above 0.4 K<sup>13)</sup>. To elucidate the bulk magnetic properties of monocrystalline Pr, a number of susceptibility, magnetization, and heat capacity measurements have also been performed. Some of

---

<sup>14)</sup> J.W. Cable, R.M. Moon, W.C. Koehler, and E.O. Wollan, Phys. Rev. Lett. 12, 553 (1964).

these experiments<sup>15)</sup> were interpreted in terms of an antiferromagnetic state whereas others<sup>16)</sup> showed no signs of magnetic ordering above 0.1 K. Pr is a singlet ground state system with weak exchange interactions and in this system ordering can only occur if the ratio of exchange to crystal field splitting exceeds a critical value. An exchange-induced ordering is believed to be accompanied by a soft mode in the excitation spectrum.

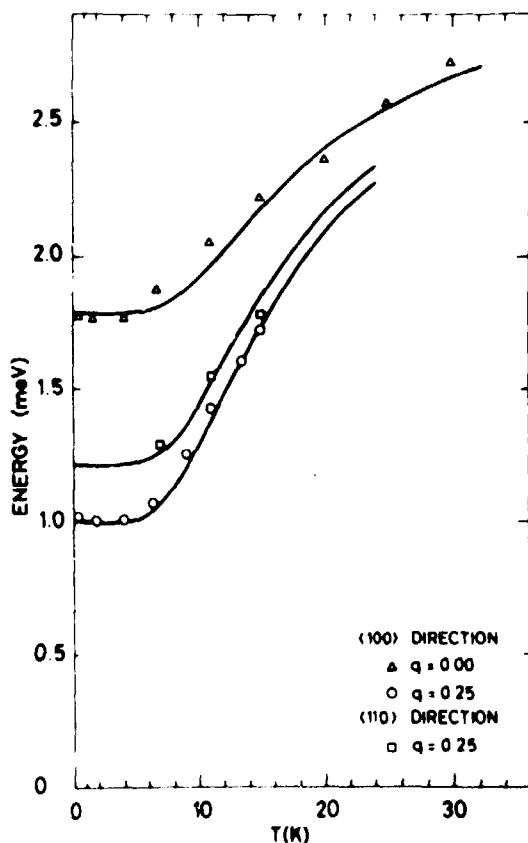


Fig. 4. Temperature dependence of selected magnetic excitations in Pr. The full lines are calculated in the RPA approximation.

<sup>15)</sup> K. Andres, E. Bucher, J.P. Maita, L.O. Longinotti, and R. Flukiger, Phys. Rev. B 6, 313 (1972).

<sup>16)</sup> P.E. Gregers-Hansen and G R. Pickett, to be published.

The minimum in the dispersion relation occurs along  $\Gamma M$ , at a point in  $\kappa$ -space ( $q \sim 0.25 \text{ \AA}^{-1}$ )<sup>10)</sup> that corresponds very closely to the modulation vector,  $Q$ , describing the magnetic order of dilute Pr-Nd alloys<sup>13)</sup>. This mode may therefore be considered as the incipient magnetic soft mode in Pr. The temperature dependence of this mode, the low energy mode at  $\Gamma$  and that of minimum energy between  $\Gamma$  and  $K$  have been studied at temperatures down to 0.4 K and the results are shown in fig. 4. The incipient soft mode has indeed the most rapid temperature variation at higher temperatures, but below 7 K neither it nor any other excitation decreases appreciably in energy as the temperature is reduced to 0.4 K.

In a simple random-phase approximation where the dispersion of the modes is neglected, the temperature dependence of the excitations is given by equation (1).

$$E_{\pm\gamma=x,y}^2 = \Delta^2 - \alpha^2 \cdot \Delta \cdot R(T) \times (J^Y(\bar{q}) \pm |J'^Y(\bar{q})|) \quad (1)$$

where  $\Delta$  is the crystal field splitting between  $|0\rangle$  and  $|\pm 1\rangle$ ,  $\alpha$  the matrix element of  $J^+$  or  $J^-$  between these states, and  $J(\bar{q})$  and  $J'(\bar{q})$  are the Fourier transforms of the exchange parameters. The four branches of the dispersion relations correspond to acoustic and optical modes each with  $J_x$  and  $J_y$  excitations.  $R(T)$  is a temperature renormalization factor which is just the difference in Boltzmann population factors between the ground and excited states i.e.

$$R(T) = n_0 - n_1 = (1 - \exp(-\Delta/kT)) \times (1 + 2\exp(-\Delta/kT))^{-1}. \quad (2)$$

The temperature dependence of the excitations calculated from equation (1) is plotted in fig. 4 for a  $\Delta$  of 3.2 meV and values of the exchange which give agreement with the low-temperature limit of the energies. The simple RPA approximation gives an excellent account of the temperature dependence of these modes. These results allow us to deduce that the exchange is approximately 90% of that which would be required to drive the energy of the soft mode to zero. A refined calculation<sup>17)</sup> in which the

<sup>17)</sup> P.-A. dgård, p. 27.

dispersions of the modes is taken into account shows qualitative agreement with the present results and gives a  $\Delta$  of 3.75 meV and a value of the exchange which is 93% of the critical value.

The effect on the excitons of an applied magnetic field was also studied. Fields up to 4.5 T were applied in both the  $\langle 100 \rangle$  and the  $\langle 110 \rangle$  directions. Fig. 5 shows the results for the  $\langle 100 \rangle$  direction with the field applied along  $\langle 110 \rangle$ . We observe

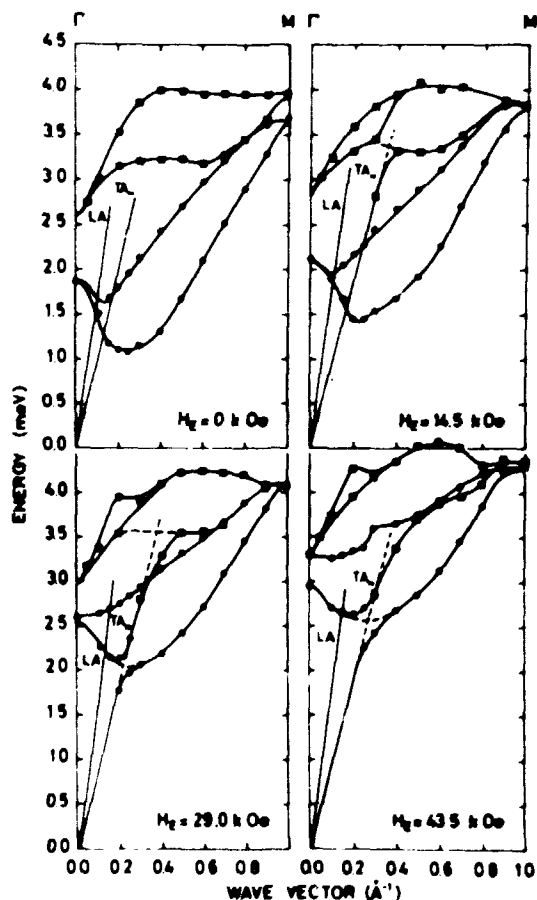


Fig. 5. Field dependence of the exciton energies and of the exciton-phonon interactions for excitons propagating in the  $\langle 100 \rangle$  directions in Pr at 4.2 K. The field is applied along the  $\langle 110 \rangle$  direction.

very large changes in the exciton energies, especially the low energy excitons. We also observe a large field dependent exciton-phonon interaction. The results have not yet been analysed in detail but selection rules determined by Jensen<sup>18)</sup> are in complete agreement with our observations. In the  $\langle 100 \rangle$  direction we observe interactions between the  $TA_{||}$  phonons and the acoustic and optical  $J_x$  excitations, as well as between the LA phonon and the acoustic  $J_y$  excitations.

A detailed analysis of the results is being undertaken, and it is also planned to study the temperature dependence of the exciton modes in a Pr-5% Nd crystal that orders antiferromagnetically on the hexagonal sites at 6.5 K.

### Theory of Magnetic Excitations in Pr

(P.-A. Lindgård)

The  $Pr^{3+}$  ions at the hexagonal sites in dhcp Pr are an example of an ideal  $S = 1$  model system with a single<sup>+</sup> ground state. The measured exciton dispersion curves have been analysed and show a significant two-ion-anisotropy of the Kaplan-Lyons type. Using a parametrization of the dispersion relations on a basis of real space exchange constants, it is possible to deduce the crystal field splitting  $\Delta = 3.74$  meV and the dispersion surface at any wave vector. A self-consistent RPA theory for the temperature dependence of the excitons has been developed. Because of the simplicity of the  $S = 1$  system, it is possible to find the renormalization constant  $Q(T)$  by taking into account the exciton scattering at all wave vectors. We find

$$Q(T) = -\frac{1}{2}(3\langle S_z^2 \rangle - S(S+1)) = -2 \times \left\{ 1 + \frac{3}{N} \sum_q \frac{\Delta}{E_q(T)} \coth\left(-\frac{E_q(T)}{2kT}\right) \right\}^{-1},$$

where  $E_q(T)$  is the renormalized exciton energy. If the dispersion is neglected  $Q(T)$  reduces to the difference between the population factors of the  $|0\rangle$  and the  $|1\rangle$  levels. From the dispersion relation the critical ratio of exchange interaction to crystal field is found to be  $0.93 < 1$  in agreement with that

---

<sup>18)</sup> J. Jensen, p. 28.

found from the Pr-Nd alloy transition temperatures<sup>13)</sup>. As also  $Q(0)$  is found to be 0.93 the conclusion is that zero point motion prevents the occurrence of ordering. The analysis of the two-ion anisotropy shows directly that it is of pseudo-multipole nature, i.e. the interaction depends on the projection of the moment onto the vector connecting the two ions. It is not a crystal field induced anisotropy as for example the Ising interaction in  $\text{TbLiF}_4$ .

#### Coupling between the Magnetic Excitations and the Phonons in Pr (J. Jensen)

The magnetic excitations propagating on the hexagonal sites of dhcp Pr are observed to be strongly coupled to the phonons when an external magnetic field is applied in the basal plane<sup>10)</sup>. At zero field no coupling is observed.

The selection rules for the linear couplings between the phonons and the magnetic excitations of the hexagonal ions propagating along the symmetry directions have been determined. The selection rules were deduced for the field applied along an a- and along a b-direction. In the calculation we neglected the presence of the ions on the cubic sites and all other crystal field levels except those describing the magnetic excitations in zero field (the ground state,  $|0\rangle$ , and the doubly degenerate first excited state,  $|1\rangle$ ). As an example we show in table I the coupling scheme derived for the modes propagating along the b-direction perpendicular to a field applied along an a-direction.

The strongest coupling which has been observed in Pr is the interaction between the "acoustic transverse" phonon and the exciton modes ( $\text{TA}_x\text{-EA}_y$ ) appearing as an energy gap at the nominal crossing point of the unperturbed dispersion relations. At 4.2 K the energy gap was found to be proportional to the internal field, as predicted, reaching a value of about 1 meV at an applied field of 5 T. At this field we deduced that the corresponding elastic constant ( $c_{66}$ ) should be reduced by 15% from its zero field value.

	LA	TA <sub>x</sub>	TA <sub>z</sub>	LO	TO <sub>x</sub>	TO <sub>z</sub>
EA <sub>x</sub>	H		O	H		O
EA <sub>y</sub>		H			H	
EO <sub>x</sub>	H		O	H		O
EO <sub>y</sub>		H			H	

Table I. The selection rules for the coupling between excitons and phonons propagating in the b-direction of Pr perpendicular to a field applied along an a-direction. The (x,y,z)-system is defined to coincide with an (a,b,c)-axis system of the hexagonal lattice. EA<sub>i</sub> denotes the (acoustic) exciton polarized along the i-axis (longitudinal mode), etc. For TA<sub>i</sub> the subscript i denotes the direction of the polarization vector of the (acoustic) transverse phonon. In the scheme O indicates that the couplings may be present in zero field, whereas H means a coupling which at low fields is proportional to the internal field.

#### The Magnetic Form Factor of Pr-26% Nd

(P.Aa. Hansen and B. Lebech)

Neutron diffraction measurements have shown that dhcp Pr metal is magnetically disordered above 0.4 K. However, a sizable magnetic moment may be induced by applying a magnetic field along a  $\langle 100 \rangle$  reciprocal lattice vector. It is therefore possible to measure the magnetic form factor of Pr by the polarised neutron technique at scattering vectors with non-zero Bragg intensity. From such measurements it was found<sup>19)</sup> that the experimental form factor is more sharply peaked towards small scattering vectors than that calculated using the non-relativistic radial integral of Blume, Freeman, and Watson. Because of this it would be valuable to measure the form factor in the forward direction. This is not possible using the polarised neutron techniques.



$\text{Pr}_{1-x}\text{Nd}_x$  ( $x > 0.03$ ) has a modulated magnetic structure at low temperatures similar to that observed in Nd. This magnetic structure gives rise to additional Bragg scattering (magnetic satellites) around the reciprocal lattice points generated by the hexagonal Bravais lattice. It might be possible to deduce the form factor of Pr even at small scattering vectors from the intensity of magnetic satellite peaks observed in an alloy. The form factor deduced from such measurements on a Pr-26% Nd (fig. 6) crystal are neither consistent with the earlier measurements of the Pr form factor nor with a calculation of the form factor based on the Blume, Freeman, and Watson radial integral. This seems to indicate that the form factor depends strongly on the surroundings of the ions. Similar measurements on a dilute alloy of Pr-Nd may therefore be valuable.

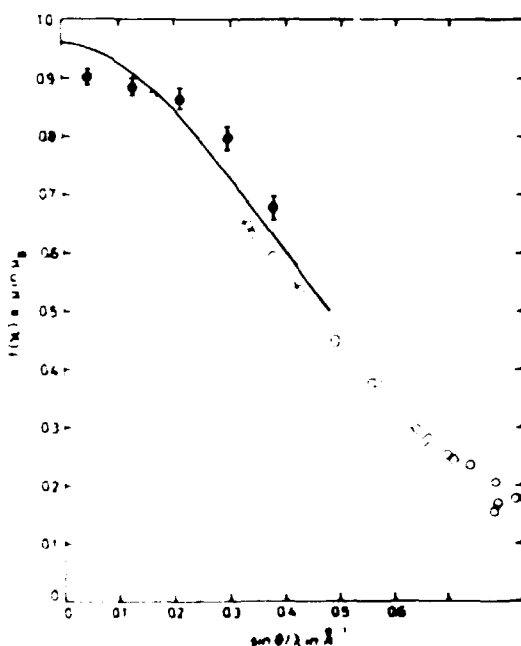


Fig. 6. The magnetic form factor  $f(k)$  of Pr (○) determined by polarized neutron scattering compared to the magnetic form factor of Pr-26.3% Nd (●) determined by Bragg scattering of neutrons. The solid line shows the  $\mu \cdot f(k)$  of Pr calculated in the dipolar approximation using the BFW wave function and the bulk magnetization value  $0.96 \mu_B$  of the Pr moment per site.

### Crystal Fields in Er-98% Y Studied by Neutron Scattering

(C. Rathmann, J. Als-Nielsen, and P. Bak)

The splitting of the  $J = 15/2$  multiplet of Er in an hcp crystal field has been determined by inelastic neutron scattering from a single crystal of Er-98% Y. Least squares fits to the spectra gave crystal field parameters  $B_{20} = (-0.34 \pm 0.04) \text{ K}$ ,  $B_{40} = (0.7 \pm 0.2)10^{-3} \text{ K}$ ,  $B_{60} = (0.21 \pm 0.02)10^{-4} \text{ K}$ , and  $B_{66} = (-0.30 \pm 0.03)10^{-3} \text{ K}$ , in good agreement with results derived from the bulk magnetization measurements of Høg and Touborg<sup>20)</sup>. In the crystal field level scheme the first excited state at 2.2 meV showed a significant energy broadening of 1.0 meV (full width at half maximum). It seems likely that this energy broadening is caused by the indirect exchange interaction between neighbouring Er ions.

### Crystal Field Parameters and Phase Transitions in ErSb

(S.M. Shapiro and P. Bak)

In most rare earth pnictides the magnetic ordering is accompanied by a structural phase transition. In the various systems studied the magnetic and structural transitions occur at the same temperature. ErSb has not been as extensively studied as other members of the series. In an attempt to gain a more complete understanding of the magnetic properties and the phase transition we investigated the crystal field levels of the Er ion and the behaviour of the spontaneous magnetization in the vicinity of the Néel temperature,  $T_N = 3.55 \text{ K}$ , using neutron scattering techniques.

The crystal field parameters obtained are

$$A_4 \langle r^4 \rangle = (106 \pm 1) \text{ K} \text{ and } A_6 \langle r^6 \rangle = (2.9 \pm 0.3) \text{ K}.$$

---

<sup>20)</sup> J. Høg and P. Touborg. *Phys. Rev. B* **10**, 2920 (1974).

These parameters are distinctly different from those obtained from specific heat measurements on ErSb and through interpolation from measurements on other similar rare earth compounds. They are considerably higher than the values for ErP, revealing the limitations of the simple effective point charge model.

The phase transition was found to be of second order in contradiction to the interpretations of the specific heat measurements. No changes in position of Bragg peaks below and above  $T_N$  were found, implying that the change in lattice parameters is less than 0.1%.

#### Crystal Field Splitting in NdN

(P. Bak and E. Warming)

The crystal field levels of the Nd ( $J = \frac{9}{2}$ ) ion in NdN have been determined by inelastic neutron scattering. The crystal field parameters obtained by a least squares fit to the spectra at 80 K are:  $B_4 = (-0.042 \pm 0.002)$  K and  $B_6 = (-0.00042 \pm 0.00002)$  K. The level sequence is the same as for the other Nd-monopnictides and monochalcogenides. The ground state is a  $\Gamma_8^{(2)}$  quartet, separated 63 K and 141 K from a  $\Gamma_5$  doublet and a  $\Gamma_8^{(1)}$  quartet respectively. The fourth and sixth order terms in the crystal field Hamiltonian can be accounted for by effective point charges of -1.2 and -3.8, respectively. These values have been obtained using the non-relativistic Hartree Fock radial integrals  $\langle r^n \rangle$  tabulated by Blume, Freeman, and Watson for easy comparison with the analysis of Birgeneau et al.<sup>21)</sup> We find that our result deviates significantly from the "universal curve" which seems to be valid for the RE(P, As, Sb, Bi) compounds, predicting an effective charge of -2 for the fourth order parameter in NdN. Moreover, the point charge value -1.2 is in clear disagreement with the value -3 determined by Davis and Mook<sup>22)</sup> for PrN.

---

<sup>21)</sup> R.J. Birgeneau, E. Bucher, J.P. Maita, L. Passell, and K.C. Turberfield, Phys. Rev. B 8, 5345 (1973).

<sup>22)</sup> H.L. Davis and H.A. Mook, AIP Conf. Proc. 10, 1548 (1972).

## Crystal Fields in Rare Earth $Al_2$ Compounds

(P. Bak)

The efforts to determine the crystal field splittings in rare earth  $Al_2$  compounds by analysing neutron scattering and magnetization experiments were continued<sup>23)</sup>. The ground state of the Pr ion in  $PrAl_2$  is a non-magnetic  $\Gamma_3$  doublet giving rise to a van Vleck type of magnetic ordering analogous to the ordering in singlet ground state systems. The lower states of Tb in  $TbAl_2$  are a  $\Gamma_1$  singlet and a  $\Gamma_4$  triplet with an energy separation of 7 K. This level scheme accounts for the concentration dependence of the thermopower anomaly and the superconducting transition temperature in  $La_{1-x}Tb_xAl_2$ . By comparing crystal field parameters for several  $Al_2$  compounds it was found that a simple effective point charge generally reproduces both the fourth order and the sixth order parameters within 30%.

## Crystal Field Theory Including Fluctuations in the Molecular Field

(P.-A. Lindgård)

The calculation of magnetic properties of systems in which the crystal field dominates the exchange interaction is generally made by considering an effective single ion free energy  $F_{MF}$ . The exchange interaction is included as an average molecular field. However, we know from general statistical mechanics that the true free energy is lower,  $F \leq F_{MF}$ . A better approximation than  $F_{MF}$  may be found by including the fluctuations. This is done by means of perturbation theory when treating the pair interaction minus the molecular field as the perturbation. To second order we find for the free energy at temperature T

$$F_{\text{corr.}} = F_{MF} - kT \sum_R \sum_{\alpha} \frac{(J_R^{\alpha})^2}{(g\mu_B)^4} (x^{\alpha\alpha})^2 \quad (1)$$

<sup>23)</sup> P. Bak, Risø Report No. 312 (1974), P. Bak, J. Phys. C 7, 4097 (1974), and H.-G. Purwins et al., J. Phys. C 7, 3573 (1974).

where  $\alpha = x, y, z, \dots$ ,  $g_R^\alpha$  = the exchange constant, and  $\chi^{\alpha\alpha}$  = susceptibility. Any thermodynamic quantity can then be found from  $F_{\text{corr.}}$  by differentiation.

For a  $S = 1/2$  Heisenberg magnet we find that the transition temperature is lowered relative to the molecular value  $T_C = T_C^{\text{HF}}(1-1/2z)$ , where  $z$  is the number of neighbours. We have applied the theory to  $\text{TbLiF}_4$  and found that  $T_C$  is reduced by 10%. This increases the ratio between  $T_C$  determined experimentally and theoretically from 0.73 to 0.80. It is not known if additional terms in the expansion (1) can provide agreement.

#### The Dipolar Coupled Ising Ferromagnet $\text{LiTbF}_4$

(J. Als-Nielsen, L.M. Holmes (Laboratorium für Festkörperphysik ETH, Zürich), and H.J. Guggenheim (Bell Laboratories, U.S.A.))

The magnetic interactions in  $\text{LiTbF}_4$  have been studied by measurements of the quasi-elastic scattering of neutrons from the paramagnetic crystal. Scattering data have been collected at 18.6 K, a temperature that is 6.5 times the Curie temperature  $T_C$ , of  $\text{LiTbF}_4$ . These data have been least squares fitted to an expression for the scattering cross section which includes, in addition to the dominant dipolar coupling, two exchange parameters  $\phi_1$  and  $\phi_2$  describing the non-dipolar coupling between nearest- and next-nearest-neighbour  $\text{Tb}^{3+}$  ions, respectively. The derived exchange parameters are  $\phi_1/k = (-0.26 \pm 0.09)$  K and  $\phi_2/k = (+0.05 \pm 0.10)$  K. Based on these parameters the total interaction energy for nearest-neighbour ions is  $\frac{4}{3}$  dipolar and  $-\frac{1}{3}$  non-dipolar. For second neighbours the non-dipolar interactions are less important. The wave vector dependent susceptibility,  $\chi_\alpha(\underline{Q})$ , was derived in the mean-field approximation, and the dipolar interactions were evaluated numerically using Ewald's technique.

The spatial correlations near  $T_c$  have been studied by small angle neutron scattering. The correlation range,  $\xi$ , exhibits Landau behaviour,  $\xi = 2.05 \times (T/T_c - 1)^{(0.48 \pm 0.02)} \text{ \AA}$ , as predicted by Wilson renormalization group analysis. Resolution problems associated with the confinement of the susceptibility  $\chi_{T \rightarrow T_c}(Q)$  to wave vectors perpendicular to the Ising axis were investigated in detail.

The spontaneous magnetization  $\mu$  below  $T_c = 2.873 \text{ K}$  was measured by magnetic Bragg scattering of neutrons. The data were normalized by comparing the magnetic Bragg scattering to the nuclear Bragg scattering at  $T > T_c$ . The nuclear structure factors as well as the extinction corrections were determined at 295 K and 100 K by conventional neutron structure analysis from 304 and 196 non-symmetry related Bragg reflections, respectively. In the critical region  $0.001 < 1 - T/T_c < 0.034$  the data obeyed the power law  $\mu = (18.5 \pm 1.5) \times (1 - T/T_c)^{(0.46 \pm 0.02)}$ . The saturation moment is  $8.9 \mu_B$ .

#### Nuclear and Electronic Antiferromagnetism in $\text{HoPO}_4$

(J. Als-Nielsen, G. Pepy (Saclay, France) and M. Chapellier)

The strong hyperfine coupling of Ho implies a significant nuclear spin ordering at temperatures below approximately 0.5 K. This effect is well known from e.g. specific heat data at low temperatures in the rare earth compounds, but it has never been observed by a direct diffraction experiment. We have utilized the fact that  $\text{HoPO}_4$  is an Ising system with the magnetic moment of the 4f-electrons along the z-axis of the tetragonal unit cell. Therefore there is no contribution to the elastic magnetic scattering from the 4f-moment when the wave vector transfer is along the z-axis. Thus any intensity in the (002) reciprocal lattice point must originate solely from antiferromagnetic ordering of the nuclear spins. By neutron diffraction on single crystals of  $\text{HoPO}_4$ \* we have observed the temperature dependence of the (002) magnetic Bragg reflection in the region  $0.4 < T < 1.4 \text{ K}$  using a

---

\*The  $\text{HoPO}_4$  crystals were grown by Knud Brodersen, Chemistry Department.

pumped  $^3\text{He}$  cryostat. The data is consistent with the expected antiferromagnetic nuclear ordering. The 4f spontaneous magnetization has also been measured versus temperature, using the (011) reflection.

#### Magnetic Properties of $\text{MnNb}_2\text{O}_6$

(B. Lebech, S.V. Nielsen (The Technical University of Denmark), and L.M. Holmes (Laboratorium für Festkörperphysik, ETH, Zürich))

The chemical structure of  $\text{MnNb}_2\text{O}_6$  is orthorhombic ( $D_{2h}^{14}$  - Pbcn) with four formula units per unit cell. In this structure the  $\text{Mn}^{2+}$  ions are situated in layers perpendicular to the a-axis with an inter-layer distance of 7.2 Å and a nearest neighbour  $\text{Mn}^{2+}$  distance of 3.4 Å. The compound orders antiferromagnetically below 4.3 K. Previous neutron diffraction measurements on powdered samples<sup>(24)</sup> suggest a spin arrangement parallel to the a-axis. However, the powder data are not sufficient for an unambiguous determination of the magnetic structure.

We have completed a neutron diffraction study of single crystals grown from the melt. A preliminary analysis of the diffraction data obtained between 4.3 and 1.2 K reveals a collinear magnetic structure but the spins are not parallel to the a-axis. We have also measured the magnetic susceptibility in the temperature range 1.6-30 K in fields up to 6 T. From 1.6 to 3.8 K a spin flip is induced by fields of 1.7-2.1 T applied in the a-direction. Furthermore, elements of the magnetic susceptibility tensors up to rank 1, have been determined. These elements are in fair agreement with a magnetic anisotropy originating solely from magnetic dipolar interactions. However, the observed spin flop field only amounts to about half the value calculated from magnetic dipolar interactions. Therefore, a neutron diffraction study of the spin-flopped phase has been initiated. Because the dipolar interactions are very sensitive to the  $\text{Mn}^{2+}$  positions, we intend to refine the nuclear structure using room temperature neutron diffraction data.

---

<sup>(24)</sup> H. Weitzel, Z. Anorg. Allg. Chemie 380, 119 (1971).

Spin Wave Dispersion and Sublattice Magnetization in  $\text{NiCl}_2$   
(P.-A. Lindgård, R.J. Birgeneau<sup>\*</sup>, J. Als-Nielsen, and  
H.J. Guggenheim<sup>\*</sup> (<sup>\*</sup>Bell Laboratories, U.S.A.))

The spin wave dispersion and sublattice magnetization data have been reanalysed on the basis of the spin wave theory by Lindgård and Danielsen<sup>7)</sup>. The temperature dependence is accounted for up to 40% of  $T_N$  using no adjustable parameters. The specific heat and density of states were also calculated.

Excitations in a Two-Dimensional Random Antiferromagnet  
(R.J. Birgeneau<sup>\*</sup>, L.R. Walker<sup>\*</sup>, H.J. Guggenheim<sup>\*</sup> (<sup>\*</sup>Bell Laboratories, U.S.A.), G. Shirane (Brookhaven National Laboratory, U.S.A.), and J. Als-Nielsen<sup>†)</sup>)

Observations were made of two well-defined bands of propagating excitations in an inelastic scattering study of the magnetic excitations in the planar Heisenberg random antiferromagnet  $\text{Rb}_2\text{Mn}_{0.5}\text{Ni}_{0.5}\text{F}_4$  at 7 K. A simple random alloy model is found to predict accurately the measured dispersion relations using essentially the pure crystal parameters for  $\text{Rb}_2\text{MnF}_4$  and  $\text{Rb}_2\text{NiF}_4$  while the zone boundary energy widths are well accounted for by an Ising cluster model. The observed intensities, however, are not properly explained using these simple models.

---

<sup>†)</sup> Work performed as a summer guest at Brookhaven under the auspices of the U.S. Atomic Energy Commission.



# Canonical Bands of Metals

(O. Jepsen and O. Krogh Andersen)

The electronic energy bands of metals can be simply described in terms of potential parameters and canonical structure constants<sup>25)</sup>  $S_{lj;l'j'}^k$ , which in contrast to the KKR structure constants are independent of energy and atomic volume. We have computed and tabulated the canonical structure constants for the fcc, bcc, and hcp ( $c/a = 1.673$  and  $1.580$ ) structures throughout the corresponding Brillouin zones. The diagonal elements  $S_{lj}^k$ , named canonical bands, are shown in fig. 7 for the bcc structure along the lines of high symmetry.

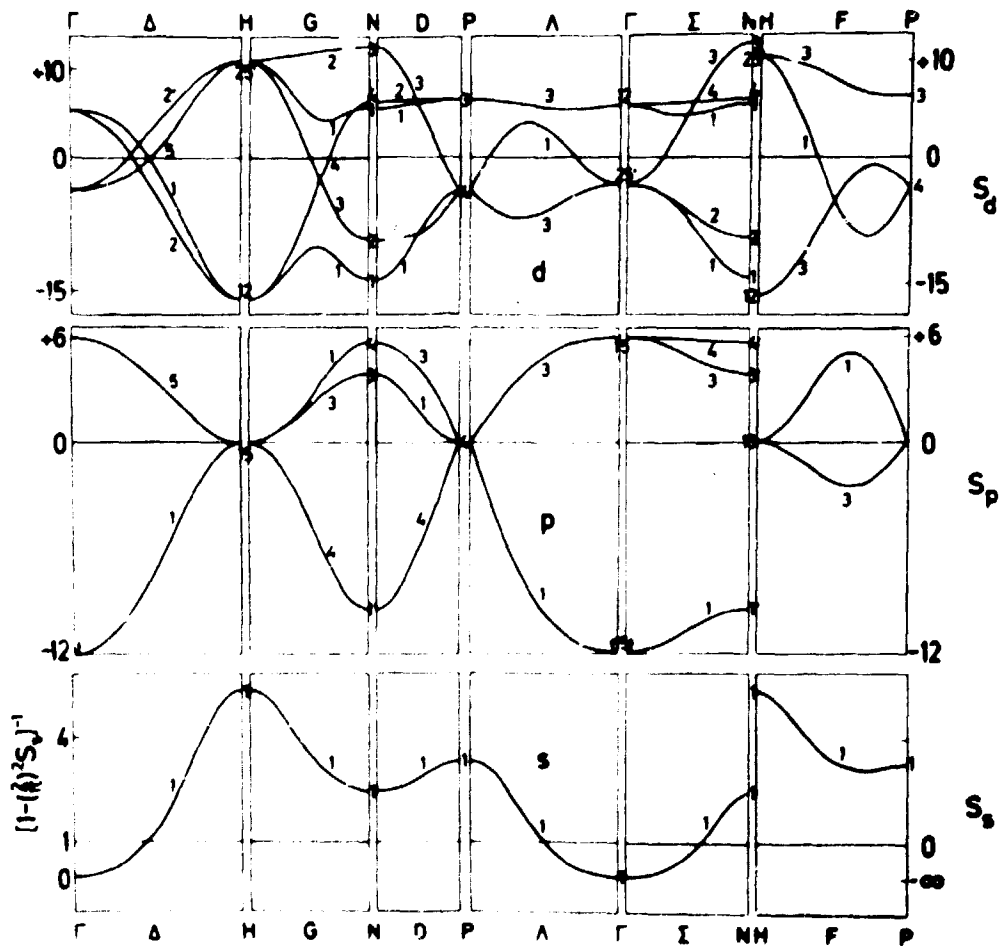


Fig. 7. The canonical s-, p-, and d-bands for the bcc-structure.

<sup>25)</sup> O. Jepsen and O. Krogh Andersen, Phys. Report No. 300, 30 (1973) and O. Krogh Andersen, Solid State Commun. 13, 133 (1973).

# Potential Parameters of Metals

(O. Jepsen and Krogh Andersen)

The potential parameters govern the positions and widths of the energy bands relative to those of the canonical bands and they also determine the strength of hybridization. We have computed these parameters for all simple, alkaline earth, transition, and noble metals using muffin-tin potentials constructed by superposition of atomic charge densities and using full Slater exchange. This construction has so far been the most successful for computation of Fermi surfaces. Together with the canonical bands this tabulation of the crystal potential parameters summarizes in a convenient way our present knowledge about the electronic energy bands of metals.

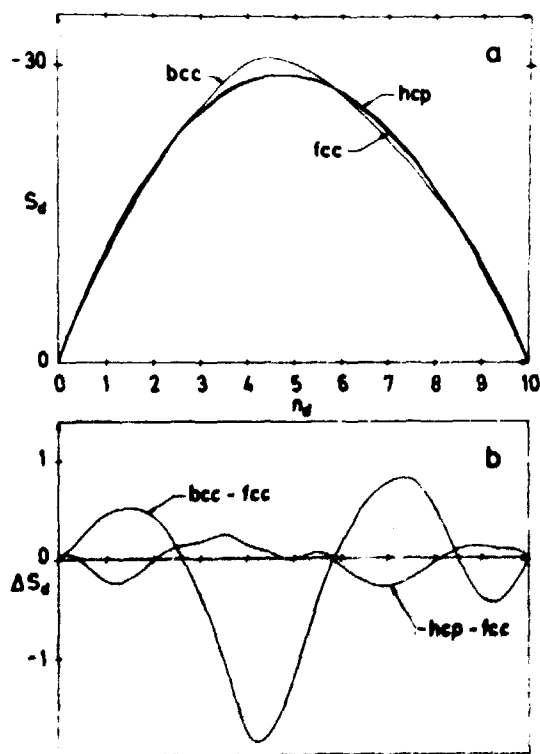


Fig. 8. The total energies (a), and the differences of total energies (b), as function of d-band occupancy ( $n_d$ ) for the fcc-, bcc-, and hcp-structures.

### Crystal Structures of Transition Metals

(O. Jepsen and O. Krogh Andersen)

We have used the fcc, bcc, and hcp canonical d-bands to compute the differences of total energies at  $T = 0$  K as function of d-band occupancy. The result shown in fig. 8 correctly predicts the observed structures except for Pd and Pt ( $n_d \approx 9.5$ ), which are fcc rather than bcc. The origin of this discrepancy, which was also found by Pettifor<sup>26)</sup>, is currently being investigated.

### The Electronic Structure of hcp Transition Metals

(O. Jepsen, O. Krogh Andersen, and A.R. Mackintosh)

The electronic energy bands of the hcp transition metals Ru, Os, Zr, and Hf have been calculated by Andersen's method<sup>25)</sup> including the non-spherical contribution to the cellular potential and all relativistic effects.

The d-bands narrow and decrease in energy relative to the sp-bands on moving along the transition series (i.e. from Zr/Hf to Ru/Os) or from the 5-d to the 4-d elements (i.e. from Hf/Os to Zr/Ru). From the energies in 396 points in the irreducible Brillouin zone the state densities and Fermi surfaces have been calculated by the analytic tetrahedron integration method<sup>27)</sup>. The calculated Fermi surfaces of Ru and Os are in good agreement with the de Haas-van Alphen experiments<sup>28)</sup> and the large areas lie within the experimental uncertainties. On the other hand there are insufficient experimental data on the Fermi surfaces of Zr and Hf to allow a detailed comparison with our calculations.

---

<sup>26)</sup> D.G. Pettifor, J. Phys. C 3, 367 (1970).

<sup>27)</sup> O. Jepsen and O.K. Andersen, Solid State Commun. 9, 1763 (1971).

<sup>28)</sup> P.T. Coleridge, J. Low. Temp. Phys. 1, 577 (1969), and  
E.N. Kamm and J.P. Anderson, Phys. Rev. B 2, 2944 (1970).

# Lattice Dynamics of $\text{Cu}_2\text{O}$

(M.M. Beg and S.M. Shapiro)

$\text{Cu}_2\text{O}$  has a simple cubic structure with two molecules per unit cell. The structure belongs to the  $O_h^4 = \text{Pn}3\text{m}$  space group. There are 18 phonon branches, 3 acoustic and 15 optical. The phonon modes at the zone centre are classified as

$$\Gamma = 3^1\Gamma_{15} + 3^1\Gamma_{25} + 3^1\Gamma_{25} + 2^1\Gamma_{12} + \Gamma_2.$$

Yu and Shen<sup>29)</sup> quoted the energies and symmetries of the optical phonons at the zone centre ( $\Gamma_{25}$ ,  $\Gamma_{12}$ ,  $\Gamma_{15}$  (TO and LO),  $\Gamma_2$ ,  $\Gamma_{25}$  and  $\Gamma_{15}$  (TO and LO)) by combining photoluminescence, infrared, and resonant Raman studies. The values quoted for  $\Gamma_{25}$  and  $\Gamma_2$  differ somewhat from those calculated in the rigid ion model by Carabatos et al.<sup>30)</sup> and from some of the results obtained by infrared and Raman techniques.

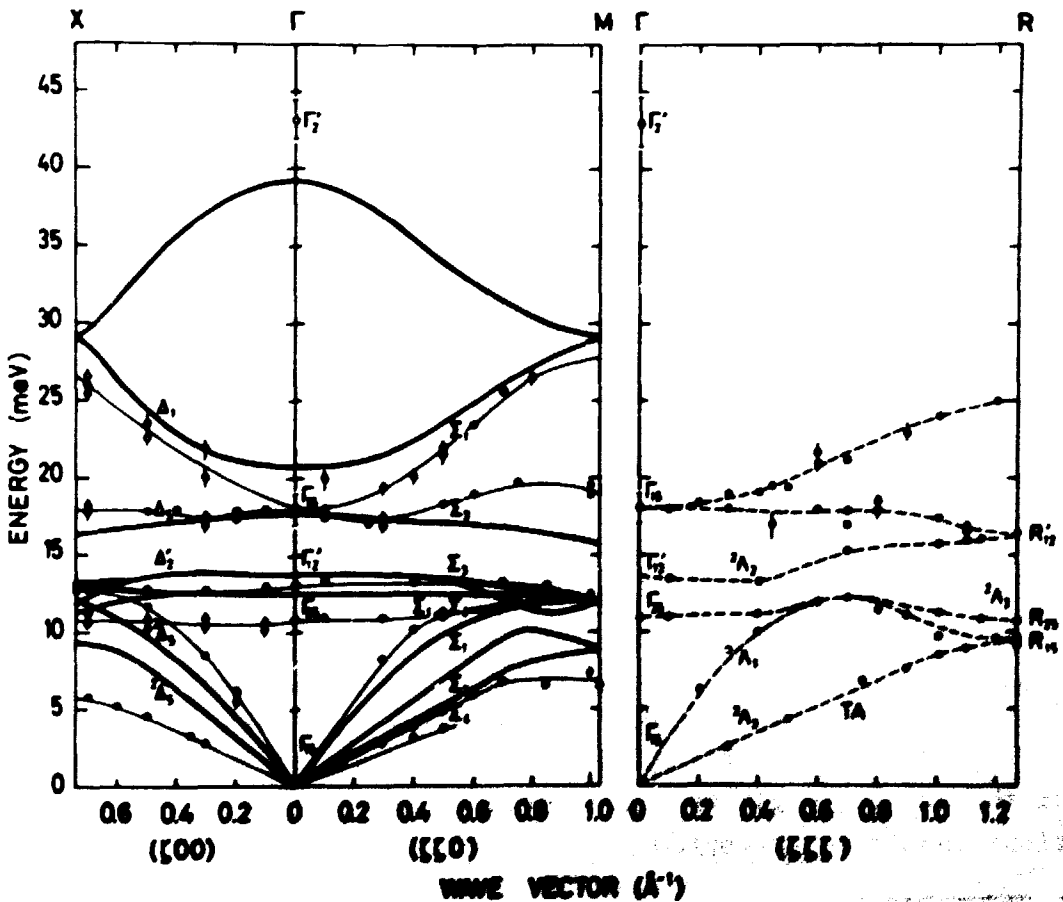


Fig. 9. Phonon dispersion relations in  $\text{Cu}_2\text{O}$  compared to the rigid ion model. The heavy lines shown in the FX and FR directions are those calculated by the rigid ion model. The thin, full and dashed lines shown in FX, FR, and FR directions are for ease of reading.

We studied the lattice dynamics of a single crystal of  $\text{Cu}_2\text{O}$  ( $\sim 1 \text{ cm}^3$ ) by inelastic neutron scattering. The crystal contained two main grains misorientated by approximately  $0.65^\circ$ . The intensity from the larger grain was twice the intensity from the smaller grain. Fig. 9 shows the phonons measured in the symmetry directions  $(\zeta, 0, 0)$ ,  $(\zeta, \zeta, 0)$ , and  $(\zeta, \zeta, \zeta)$ . Of the six optical phonon branches we were able to measure three starting from the zone centre  $\Gamma_{25}$  ( $88 \text{ cm}^{-1}$ ),  $\Gamma_{12}$  ( $110 \text{ cm}^{-1}$ ) and  $\Gamma_{15}$  ( $114 \text{ cm}^{-1}$ ). The counting statistics for phonons belonging to the branches starting from  $\Gamma_{15}$  (LO) was poor, and with the present sample it is impossible to study any higher energy branches. Efforts were made to study the branches starting from  $\Gamma_2$ , but the measurements were difficult because of low intensity and spurious peaks. However, we estimate  $\Gamma_2$  to be approximately  $43 \text{ meV}$  ( $\sim 348 \text{ cm}^{-1}$ ).

The experimental results for the  $(\zeta, 0, 0)$  and  $(\zeta, \zeta, 0)$  branches are compared with the calculation by Carabatos et al. For the acoustic modes at the zone boundary in the  $(\zeta, \zeta, \zeta)$  direction Carabatos et al. predict zero frequency, which implies an error in their calculation. Therefore comparison is not shown for that direction. Qualitatively the experimental and calculated results agree, but quantitatively there are large differences. The most important ones are the slopes of the acoustic branches, the energy of the zone centre phonons, and the split in the  $\Gamma_{15}$  ( $149$ - $153 \text{ cm}^{-1}$ ) level. Our values for the energy of zone centre phonons agree with those quoted by Yu and Shen. The preliminary values of the elastic constants obtained from the slope of the acoustic branches,  $c_{11} = (12.0 \pm 1) 10^2 \text{ N/m}^2$ ,  $c_{11} - c_{12} = (1.7 \pm 0.2) 10^2 \text{ N/m}^2$  and  $c_{44} = (1.2 \pm 0.1) 10^2 \text{ N/m}^2$  agree with the values obtained by the pulse echo technique.

Further neutron experiments perhaps using a hot source can be performed with larger and more perfect crystals. In the light of the present experiment more detailed theoretical calculations should be attempted.

<sup>29)</sup> Y. Yu and Y.P. Shen, Phys. Rev. Lett. 5, 32 (1974).

<sup>30)</sup> C. Carabatos and B. Prevot, Phys. Stat. Sol. (b) 5, 44 (1971).

### Phonons in $C_{10}D_8$

(O.W. Dietrich and G.S. Pawley (University of Edinburgh, Scotland))

Naphtalene is a comparatively simple molecular crystal. Model calculations by Pawley based on two body forces have revealed the full twelve-branch dispersion relation scheme for the molecular motions. At zero wave vector the model calculations agree fairly well with optical measurements. We have previously<sup>31)</sup> studied the dynamics of  $C_{10}D_8$  by inelastic neutron scattering. At the time, the crystal size and neutron intensity allowed us to resolve about eight branches of the dispersion spectrum. We have now repeated the measurements with a larger crystal and improved neutron intensities and have obtained all but one of the twelve branches. This will allow a refined analysis to be made.

### The Phase Transition in $C_{10}F_8$

(O.W. Dietrich and G.S. Pawley (University of Edinburgh, Scotland))

The structure of perfluoro-naphtalene,  $C_{10}F_8$ , is thought to be the same as that of naphthalene, namely monoclinic  $P2_1/c$ . It was therefore chosen for lattice dynamical study to compare with the results on  $C_{10}D_8$ . A large single crystal was grown by Dr. Sherwood (Strathclyde University, Scotland), and room temperature inelastic neutron scattering measurements were attempted. The neutron groups obtained were so broad that it was decided to make measurements at lower temperature ( $\sim 77$  K). Immediately on cooling a hitherto unknown transition occurred breaking up the crystal and rendering further inelastic measurements fruitless. However, it was found that a number of Bragg peaks were still distinguishable and it seemed that the structural aspects of the transition could be determined. Powder diffraction runs were made for both phases, but the low temperature phase was uninterpretable because two of the low index reflections overlapped.

---

<sup>31)</sup> O.W. Dietrich and G.S. Pawley, *Risø Report No. 237*, 22 (1971).

A single crystal structure analysis was therefore attempted, using a four circle diffractometer. The room temperature measurements were straightforward but have not yet been analysed. In the low temperature phase the mosaic width was about  $6^\circ$ , and great care was taken to align the crystal. This was done without any assumption of the crystal space group, and when the unit cell was calculated, two interaxial angles were so near to  $90^\circ$  that it could be deduced with considerable certainty that the cell was monoclinic. The subsequent analysis indicates that the structure is still  $P2_1/c$ . However, the unit cell dimensions and monoclinic angle have varied by as much as 10%. In the transition the molecules rotate in their planes in such a way that the interplanar spacing remains constant and the molecular plane alters only marginally. The transition is exceptional, but not unique, in that it occurs with no change of crystal symmetry. It is of first order with a temperature hysteresis of 15 K. This may not be regarded as surprising, since simple crystal energy calculations for naphthalene-type structures have shown double minima.

#### Neutron Scattering in $C_2F_6$

(B.M. Powell (Chalk River, Canada) and E. Warming)

The lattice formed by the centres of the  $C_2F_6$  molecules in the plastic phase (104 - 172 K) is bcc, with  $a = 6.038 \text{ \AA}$  at 109 K. The crystal structure contains two molecules per unit cell with some still unknown orientational and/or rotational disorder of the molecule. In the plastic phase it is rather easy to grow a single crystal of  $C_2F_6$  but it appears that the crystal is unstable. The crystal axes reorient with a temperature dependent reorientation rate.

A search for phonons or other excitations in a single crystal of  $C_2F_6$  in the plastic phase has given no result. However, inelastic neutron scattering with high energy resolution has revealed a quasielastic peak (fig. 10). The width and intensity of this peak are wave vector,  $\vec{q}$ , dependent and it has only been

observed for small  $q$ 's perpendicular to a reciprocal lattice vector. In fig. 10 is shown an energy scan at  $q = 0.15 \text{ \AA}^{-1}$  from the (110) Bragg reflection in the  $\langle 002 \rangle$  direction. (The wave vector of the incident beam was held constant at 5 meV and higher order neutrons were removed by a Be filter). The sharp peak superimposed on the wide quasielastic peak arises from incoherent elastically scattered neutrons and some Bragg scattered neutrons from the (110) reciprocal lattice point. Attempts have been made to solve the structure of the low temperature phase. Our diffraction spectra have been compared with the structure suggested by Lewis and Pace<sup>32)</sup>, but no agreement was found.

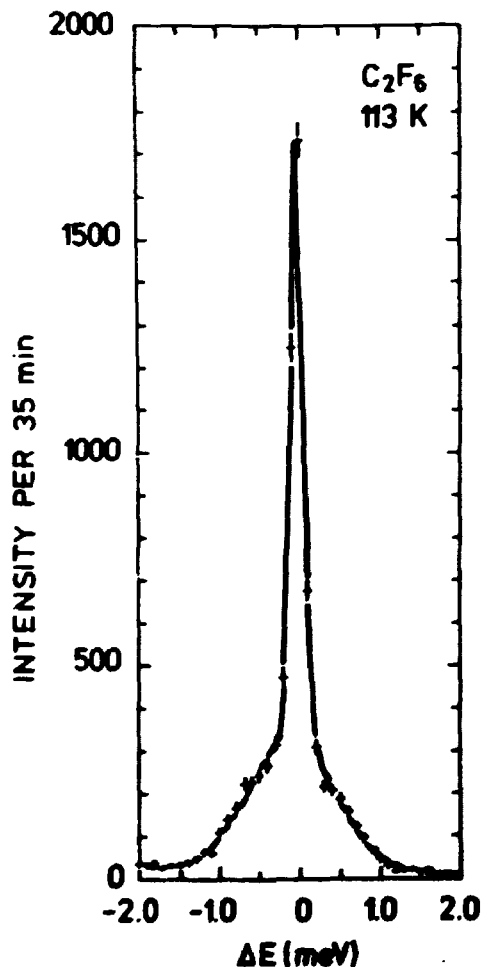


Fig. 10. Elastic and quasi-elastic peaks for  $q = 0.15 \text{ \AA}^{-1}$  from the (110) Bragg reflection in the  $\langle 002 \rangle$  direction. The full line is a least squares fit to two superimposed Gaussians.

<sup>32)</sup> A. Lewis and E.L. Pace, J. Chem. Phys. 58, 3661 (1973).



# The Structural Phase Transition in Solid DCN

(O.W. Dietrich, G.A. Mackenzie<sup>\*</sup>, and G.S. Pawley<sup>\*</sup>

(<sup>\*</sup>University of Edinburgh, Scotland))

Deuterium cyanide, DCN, forms one of the simpler molecular crystals. The molecule itself is linear and solidifies at 260 K in a body centered tetragonal structure with the molecule aligned along the tetragonal axis. At  $T_c = 160.0$  K the crystal undergoes a structural phase transition to a body centered orthorhombic structure. Lattice dynamics calculations by Rae<sup>33)</sup> have suggested that the transition is driven by a softening of the transverse sheer mode with a wave vector parallel to the base diagonal. We have carried out preliminary measurements of the structural and dynamical properties of DCN<sup>†</sup> using elastic and inelastic neutron scattering techniques. The elastic measurements have shown that the phase transition is of first order, in contrast to what was expected. However, the transition is non-destructive and a tetragonal crystal can be recovered. The inelastic measurements revealed a transverse phonon mode of extremely low energy for wave vectors parallel to the base diagonal<sup>33)</sup>. Energy scans at two vectors and for various temperatures above and below  $T_c$  are shown in fig. 11.

We have so far been unable to approach the zone center, where the softening is expected to occur, but the existence of the mode at such low energies supports the lattice dynamics calculations and Rae's suggestion of the softening mechanism as the driving force of the transition.

Our inelastic measurements have been limited to large wave vector transfers,  $q$ , because our crystals (grown from the melt) have had too large mosaic spreads to resolve the small  $q$  region. We believe the problem of growing large and low-mosaic single crystals is caused by the polymerization of DCN in long chains, which gives rise to imperfections during growth. We continue our efforts to reduce the rate of polymerization.

---

<sup>33)</sup> A.L.M. Rae, J. Phys. C 5, 3309 (1972).

<sup>†</sup> The DCN was prepared by C. Jørgensen of the Chemistry Department

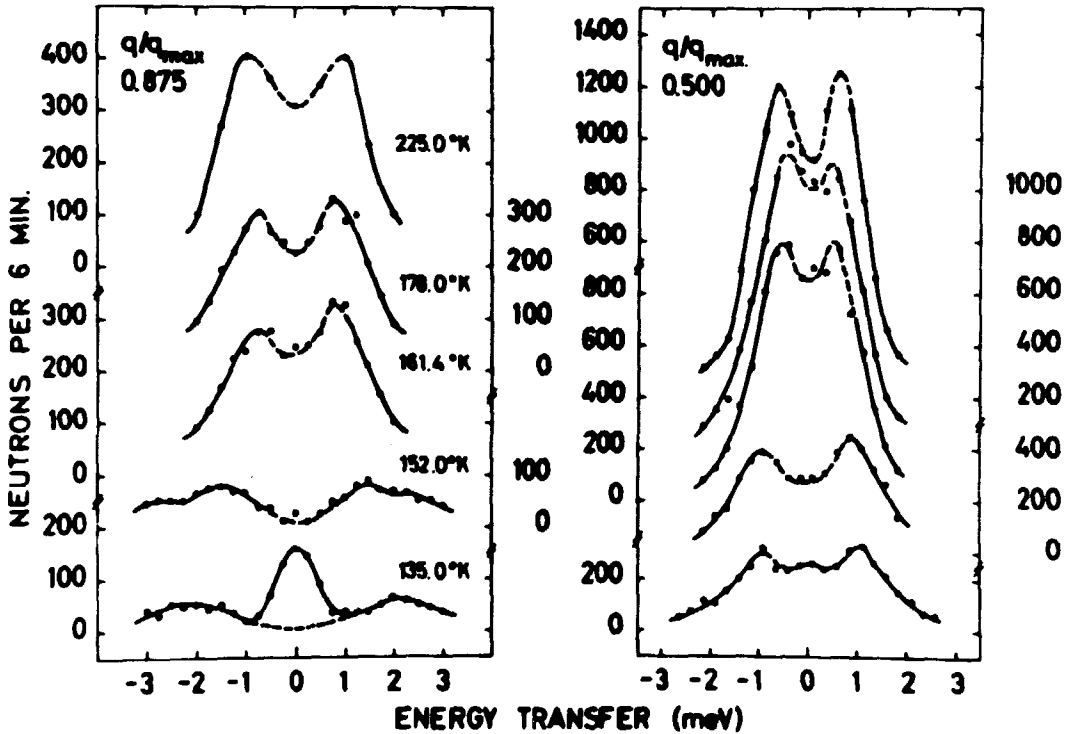


Fig. 11. Neutron inelastic scattering in DCN for two wave vectors,  $q$ , along the  $(\bar{1}10)$  direction in the Brillouin zone centered at  $(110)$ .  $q_{\max}$  corresponds to the zone boundary. The centre peak (incoherent) in the lower left intensity profile has been subtracted from the other profiles.

### Hydrogen Adsorbed on Graphite

(M. Nielsen, S. Shapiro, and W. Ellenson)

Neutron scattering experiments have been performed to study the structure and dynamics of  $H_2$  molecules adsorbed on graphite. Monolayers of para- $H_2$  molecules are adsorbed on grafoil disks which are parallel to the scattering plane of the neutrons. Grafoil is a carbon product consisting of small sheets of graphite partly oriented with their hexagonal planes parallel.

When the para- $H_2$  molecules are scattered into the  $J = 1$  rotational state by neutron scattering we observe a strong narrow line at an energy of 14.6 meV which equals the rotational energy.

This is seen in fig. 12 where some of the observed neutron groups are shown. The amount of  $H_2$  adsorbed corresponds to a monolayer of the density  $n = 0.108$  molecule/ $\text{\AA}^2$ . From the width of the observed neutron groups we conclude firstly that the splitting of the  $J = 1$  triplet is smaller than 0.3 meV and secondly that the molecules behave as a solid up to 30-40 K, or in other words that diffusion is small. From the observed intensities we may calculate the Debye-Waller factor of the molecules and we find that the mean square displacement of the molecules at 6 K is the same as in solid  $H_2$  at a pressure of about 1.5 kbar. In a neutron diffraction study of a  $D_2$  monolayer with the same amount of gas adsorbed in the grafoil filled sample cell, we find a triangular structure with a density corresponding to solid  $H_2$  at approximately 1.5 kbar.

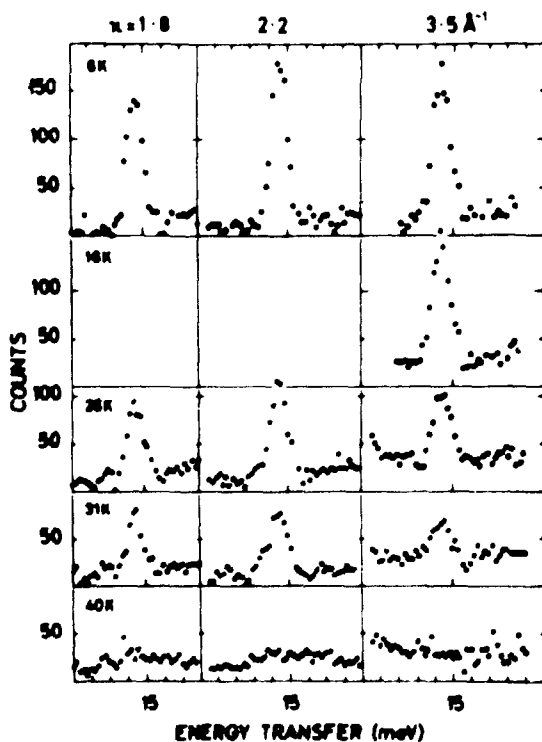


Fig. 12. Neutron groups observed by scattering from adsorbed monolayers of para- $H_2$  molecules on grafoil. The density of the  $H_2$  molecules was 0.108 molecules per  $\text{\AA}^2$  of the grafoil surface. The grafoil disks are oriented parallel to the scattering plane and the groups are observed as constant  $\kappa$ -scans using triple-axis neutron spectrometry. The scattering from the grafoil has been subtracted and the observed peaks originate from the  $J = 0$  to the  $J = 1$  scattering.

Similar results were obtained for monolayers with a density of  $n = 0.060$  molecules/ $\text{\AA}^2$ , but the mean square displacements of the molecules are larger. These results show that there exists a solid-like phase in an adsorbed monolayer of  $\text{H}_2$  on grafoil and that the molecules behave as free rotators in this phase. As the temperature increases towards 40 K the neutron scattering intensity of the  $J = 0$  to  $J = 1$  line dies out and this presumably means that the molecules gradually go into another phase. In this phase the diffusion is so fast that the neutron groups are too broad to be observed.

Neutron Scattering in Solid  $\text{H}_2$  under Moderately High Pressure  
(M. Nielsen and K. Carneiro)

Solid para- $\text{H}_2$  has been studied by neutron diffraction and by inelastic incoherent neutron scattering in the pressure range 0-2 kbar. The samples are either pressurized with  $\text{H}_2$  gas or with He gas. In the first case the maximum pressure is reached along the melting curve of  $\text{H}_2$  and the sample is cooled at constant volume. In the second case  $\text{H}_2$  is solidified in the pressure cell and the maximum pressure is reached along the melting curve of He, i.e. at 2 kbar and  $T_m = 21$  K. In this case the sample of  $\text{H}_2$  is pressurized as a powder by a piston of He. The pressures are measured with strain gauges.

The main results are:

- (1) No phase changes occur anywhere in the phase diagram up to 1.9 kbar.
- (2) The pressure dependence of volume has been measured by neutron diffraction. No changes with pressure of the c/a ratio of the hcp lattice have been detected. We find  $c/a = 1.632 \pm 0.007$ . These results agree with recent piston displacement measurements<sup>34)</sup>,

---

<sup>34)</sup> M.S. Anderson and C.A. Svenson, private communication.

i.e. measurements where the solid  $H_2$  is pressurized with a piston and the volume change determined by the piston movement.

- (3) The Debye-Waller factor has been determined at different pressures by measuring the  $J = 0$  to  $J = 1$  incoherent neutron scattering intensity as function of the scattering vector. These results are shown in fig. 13.

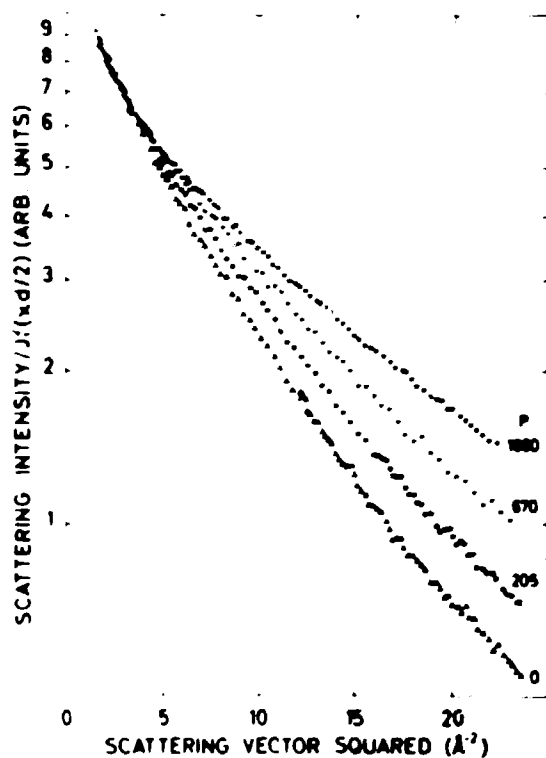


Fig. 13. Debye-Waller factor versus scattering vector squared at 5 K for  $ra-H_2$  at different pressures. The Debye-Waller factors have been derived from the intensity of the  $J = 0$  to  $J = 1$  scattering observed using triple-axis neutron spectrometry (fig. 12).

## Neutron Scattering in Liquid $H_2$

(K. Carneiro and M. Nielsen)

The coherent and incoherent scattering from liquid  $H_2$  at  $T = 14.7$  K was analysed further, giving a consistent picture of the phonons in this liquid. The observed coherent scattering was consistent with the one-phonon scattering from a system with a Debye temperature,  $\theta_D = 70$  K, and it could be analysed in terms of the one phonon sum rule to give a mean square displacement  $\langle u^2 \rangle = 0.62 \text{ \AA}^2$ . These values agree with those for the liquid when scaled according to the Grüneisen relation using the experimental value for the Grüneisen constant  $\gamma$ .

We found that the incoherent scattering was characterized by the same  $\theta_D$  and  $\langle u^2 \rangle$ , and determined a one phonon density of states  $Z(\omega)$ . This function is shown in fig. 14. For the self diffusion constant we found  $D = 4.7 \cdot 10^{-5} \text{ cm}^2/\text{s}$ . It should be emphasized that the incoherent scattering was obtained by neutron scattering from para- $H_2$ , so that multiple scattering was not possible. We believe that this fact significantly improves the quality of the observed spectra.

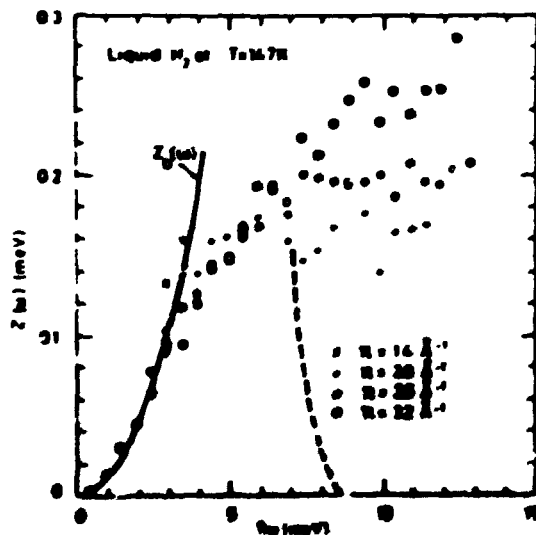


Fig. 14. Density of one phonon states  $Z(\omega)$  for liquid  $H_2$  at 14.7 K, deduced from incoherent neutron scattering.  $Z_D(\omega)$  shows the density of states derived from Debye theory. The observed Debye temperature is 70 K. The dashed line for  $\omega \approx 7$  meV indicates the rapid decrease of  $Z(\omega)$  required by the sum rule, whereas the observed scattering above 7 meV is dominated by multiphonon scattering.

# Neutron Scattering in Liquid N<sub>2</sub>

(J.P. McLague (University of California, Los Angeles)  
and K. Carneiro)

The inelastic scattering from liquid N<sub>2</sub> at 66.4 K was analysed in terms of the normalized coherent scattering law  $S_{n,coh}(\kappa, \omega)$  which is shown in fig. 15.

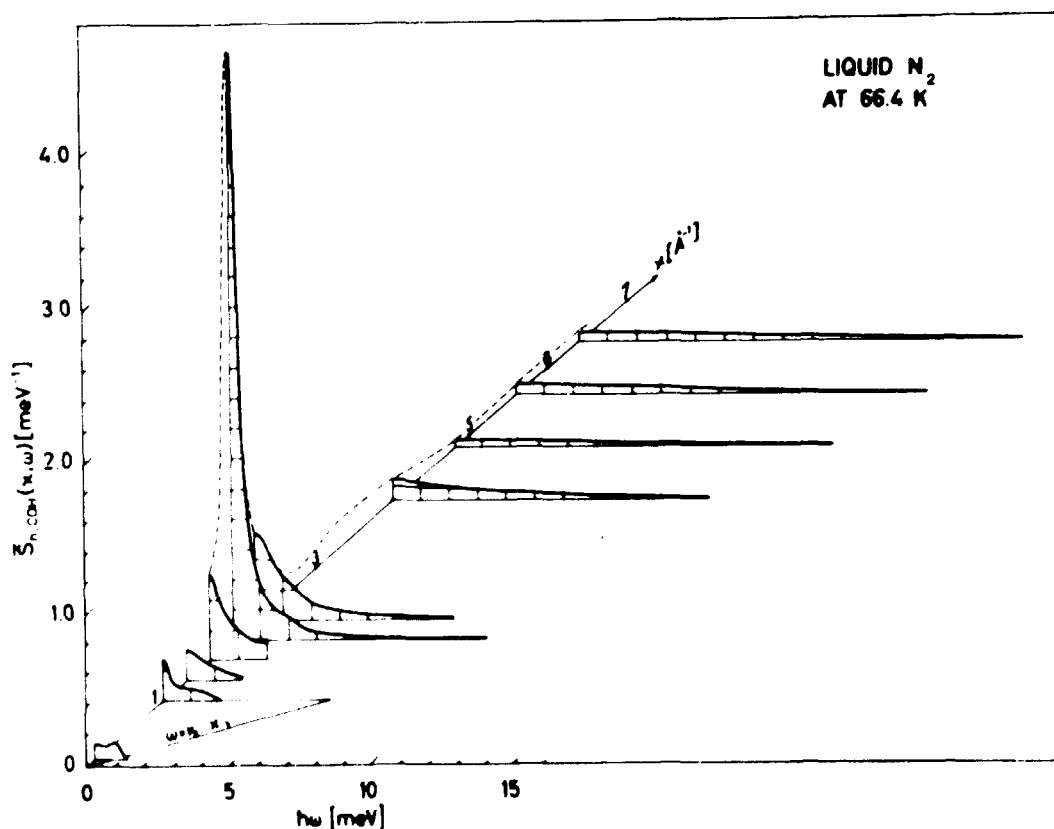


Fig. 15. Coherent scattering law for liquid N<sub>2</sub> at 66.4 K.  
At a wave vector transfer of 4.0  $\text{\AA}^{-1}$  the scattering is separated according to the formfactors in the partial wave expansion.

At small wave vector ( $\kappa = 0.1 \text{ \AA}^{-1}$ ) the spectrum shows remnants of the propagating sound mode, although the instrumental resolution in this case distorts the spectrum considerably. For  $1.0 \text{ \AA}^{-1} \leq \kappa \leq 2.2 \text{ \AA}^{-1}$  the spectra show no evidence of propagating modes. By means of the partial wave expansion, and the principle of corresponding states, we can compare the dynamics of the molecular centres of liquid N<sub>2</sub> to the dynamics of liquid Ar. An overall agreement is observed but some differences suggest that molecular anisotropy is of importance in liquid N<sub>2</sub>. At wave vectors  $4.0 \text{ \AA}^{-1} \leq \kappa \leq 6.4 \text{ \AA}^{-1}$  our spectra seem to approach

those for a gas of freely recoiling molecules. However, from the partial wave expansion, we get for the self-diffusion coefficient  $D = 1.5 \cdot 10^{-5} \text{ cm}^2/\text{s}$  in agreement with values found by other techniques. This value does not compare well with the value found for liquid A which further indicates the importance of anisotropic interactions in  $\text{N}_2$ . At these wave vectors, we can deduce the rotational diffusion coefficient  $D_r = 0.24 \cdot 10^{12} \text{ s}^{-1}$  in good agreement with other experiments.

### The Solid-Liquid Phase Transition

(J. Klæstrup Kristensen (The Technical University of Denmark) and R.M.J. Cotterill)

Although the solid-liquid phase-transition has been the subject of numerous investigations it is not completely understood. It is different from other first order transitions in that it is not possible to superheat a solid. During the last 50 years several theories have been proposed, but so far none of them have been experimentally verified.

The theories of melting can be divided into two main groups. One in which the transition is explained as a reaction starting from the surface and running through the whole crystal, and one in which the bulk crystal is supposed to be unstable with respect to the formation of a large number of defects which then break down the long range order. The following defect types have been proposed: vacancies, interstitials, and dislocations. Recent molecular dynamics computer simulations made at the Danish Technical University seem to favour the theory that melting occurs through the spontaneous generation and proliferation of dislocation loops.

To obtain information about the atomic movements involved in melting we study simple metallic solids and liquids near the transition temperature by inelastic neutron scattering. We investigate simple metals because the dislocation mechanisms in these are better understood. We mainly look for pre-melting and after-melting effects predicted by the defect-models because some of these effects have been observed in thermodynamic measurements.



So far the measurements have shown that in Al there is no abnormal change in the phonons which would be involved in the formation of Schockley-type dislocation loops as near to the melting point,  $T_m$ , as  $1/10^0$  C. However, there is some evidence of an enhanced movement of the atoms from about  $3/10^0$  C below  $T_m$ . In the liquid phase our measurements on Pb are in accordance with the theory of Schneider<sup>35)</sup>, which predicts a temperature limit for stability of the super-cooled liquid phase with respect to density fluctuations of wave vector equal to that of the principal peak in the structure factor.

#### Hydrodynamic Fluctuations near the Convection Instability in the Nematic Liquid Crystal PAA

(H. Bjerrum Møller and T. Riste (IFA, Kjeller, Norway))

The intensity of the liquid peak at  $1.8 \text{ \AA}^{-1}$  in the neutron diffraction pattern of the liquid crystal PAA (para-azoxyanisol), in its nematic phase, is a measure of the alignment of the molecules<sup>36)</sup>. The double peak, which was observed in the intensity at  $1.8 \text{ \AA}^{-1}$  versus temperature in the region of the nematic-isotropic transition, was at the time tentatively interpreted as critical scattering, associated with the stability limits of the nematic and isotropic phases respectively.

It has now been shown that these peaks decay with a time constant of several hours, and that they are caused by convective currents in the liquid, at temperature gradients exceeding a critical value. In order to study this hydrodynamic instability at the convection threshold, measurements have been made in the nematic phase at temperatures away from the complicating influence of the nematic-isotropic transition. These measurements demonstrate the similarity between this transition and the familiar second order phase transitions in, for instance, magnetism. Large fluctuations and a slowing down of the fluctuations are observed at the critical temperature gradient.

---

<sup>35)</sup> L. Schneider, Phys. Rev. A 3, 2145 (1971).

<sup>36)</sup> T. Riste and H. Bjerrum Møller, Risø Report No. 300, 38 (1971).

### Neutron Diffraction Study of Amorphous Solid Water

(Jack Wenzel, C.U. Linderstrøm-Lang (Chemistry Department), and Stuart A. Rice (University of Chicago, U.S.A.))

Olander and Rice<sup>37)</sup> have suggested that amorphous solid water may be a useful model of the liquid. We have measured the neutron diffraction spectrum from a sample of amorphous solid D<sub>2</sub>O. The sample was deposited from the vapour at 10 K. From the measured spectrum we obtained the structure factor of amorphous D<sub>2</sub>O for wave vector transfers from 0.8 - 12.3 Å<sup>-1</sup>. The results indicate that the phase investigated is truly amorphous and has a liquid-like structure factor. The Fourier transformed structure factor yields a real space pair distribution function consistent with local tetrahedral coordination and H<sub>2</sub> bonding, as in other condensed phases of water. The intramolecular OD separation is found to be 1.00 Å. The lack of data for very large wave vector transfer and the expected near equality of the intramolecular DD separation and intermolecular O...D separation make it possible to determine the intramolecular DOD angle with precision. The neutron scattering data are consistent with and complementary to the X-ray diffraction studies of Venkatesh, Rice, and Narten<sup>38)</sup>.

### Inelastic Paramagnetic Neutron Scattering in Ce Metal Under Pressure

(B. Buras, B. Lebech, and B.D. Rainford (Imperial College, London, U.K.))

At room temperature fcc γ-Ce undergoes a first order isomorphic transition to the fcc α-phase at 7 kbar. However, samples which contain mixtures of both phases at 0 kbar may be prepared. The intensity of the paramagnetic diffuse neutron scattering from

---

<sup>37)</sup> D. Olander and S.A. Rice, Proc. Nat'l Acad. Sci. U.S.A. 60, 98 (1972).

<sup>38)</sup> C.G. Venkatesh, S.A. Rice, and A.H. Narten, submitted for publication in Science (1974).

samples containing preferably  $\gamma$ -Ce or  $\alpha$ -Ce respectively at 0 kbar was first studied by Wilkinson et al.<sup>39)</sup>. Their results were interpreted in terms of a paramagnetic  $\gamma$ -phase with a localized magnetic moment originating from the 4f-electron and a non-magnetic  $\alpha$ -phase with a Pauli-type paramagnetism. Since the 4f-level in  $\alpha$ -Ce is just above the Fermi level it was suggested<sup>40)</sup> that exchange enhancement may occur at the transition. The intensity of the paramagnetic inelastic scattering is proportional to the square of the magnetic moment and the width of the inelastic paramagnetic scattering depends on both the square of the magnetic moment and on the exchange integral. Therefore, if exchange enhancement occurs at the  $\gamma$ -Ce to  $\alpha$ -Ce phase transition at 7 kbar, the width of the inelastically scattered neutrons centered at zero-energy transfer should vary.

In order to test this conclusion the pressure dependence<sup>42)</sup> of the inelastic neutron scattering from polycrystalline Ce has been studied. The incident neutron energy (14.3 meV) was kept constant and the energy distribution of the neutrons scattered inelastically under an angle of  $60^\circ$  was measured by means of a graphite analyser. Because of the low intensity of the inelastically scattered neutrons and the high background (arising mainly from the aluminium oxide pressure cell) the data taken at 0 kbar and at 20 kbar are not conclusive. A larger high pressure cell enabling the use of larger samples is under construction.

#### Pressure-Induced Phase Transition in $\text{TeO}_2$

(S. Shapiro, B. Buren, W.D. Ellenson, and T. Giebultowicz)

Feeracy and Fritz<sup>41)</sup> recently observed a pressure-induced phase transition in  $\text{TeO}_2$  at 3.0 kbar at room temperature. The transition appears to be second order and has been investigated using Brillouin-scattering, ultrasonic-velocity and dielectric-constant

---

<sup>39)</sup> M.K. Wilkinson, H.P. Child, C.J. McHague, W.C. Koehler, and E.O. Wollan, Phys. Rev. 122, 1409 (1961).

<sup>40)</sup> R. Coqblin, Colloque CNRS No. 180 Grenoble 2, 579 (1969).

<sup>41)</sup> P.S. Feeracy and I.J. Fritz, Phys. Rev. Lett. 32, 466 (1974).

measurements. The structure of the low pressure phase is tetragonal ( $D_4^4$ ). The structure of the high pressure phase was not known, but it was suggested<sup>41)</sup> that it is orthorhombic ( $D_2^4$ ).

We have initiated a neutron diffraction study of the structure of this phase using the high pressure cell<sup>42)</sup>. The preliminary results obtained by us confirm that the structure is orthorhombic. However, the structural details seem to differ slightly from the results obtained by Worlton<sup>43)</sup> using neutron time-of-flight techniques.

#### Pressure Dependence of the Néel Temperature of Cr Single Crystal (B. Buras and B. Lebech)

Electrical resistivity measurements<sup>44)</sup> showed that the Néel temperature,  $T_N$ , of Cr is pressure dependent and that  $(dT_N/dP)_{P \rightarrow 0} = 5.1$  K/kbar. The pressure dependence of the Néel temperature was studied by means of elastic neutron scattering using the high pressure cell<sup>42)</sup>. The cylindrical Cr single crystal (5.5 mm in diameter, 15 mm long) was mounted in the cell with the (110) zone axis vertical and parallel to the cylinder axis. The crystal was then oriented using the (002) nuclear reflection. The temperature dependence of the intensity of the (1-Q,0,0) magnetic satellite was followed at 0 and 2 kbar. The Néel temperature decreased by  $(9.5 \pm 1)$  K upon increasing the pressure from 0-2 kbar in agreement with the electrical resistivity data quoted above. The temperature dependence of the ordered magnetic moment close to  $T_N$  suggests that the transition under pressure is less first order than at atmospheric pressure. However, to justify this conclusion measurements with improved control of the sample temperature are required.

---

<sup>42)</sup> B. Buras, B. Lebech, W. Kofoed, and G. Bäckström, Risø Report No. 300, 44 (1973).

<sup>43)</sup> T.G. Worlton, private communication.

<sup>44)</sup> D.B. McWhan and T.M. Rice, Phys. Rev. Lett. 19, 846 (1967).

### Neutron Scattering from Crystalline Se

(F.Y. Hansen (Technical University of Denmark), W.D. Ellenson and E. Warming)

The Debye-Waller factor for crystalline Se is expected to become anharmonic at higher temperatures and in this region it is of interest to study the phonon dispersion relations. In order to determine the temperature dependence of the Debye-Waller factor we have measured a set of neutron diffraction spectra from 4.2-480 K.

The crystal structure of crystalline Se is hexagonal with 3 Se atoms per unit cell. The atoms are situated on spiral chains going through the lattice parallel to the hexagonal axis. From the set of diffraction data we have derived linear changes of the lattice parameters,  $a$  and  $c$ ;  $\Delta a = 2.7\%$  and  $\Delta c = -0.8\%$ . This shows that the lattice expands in the hexagonal plane with increasing temperature, but the dihedral bond angle in the Se-chains is only slightly distorted. This implies that the coupling forces between the chains are much weaker than the bonding forces within the chain.

### Determination of the Debye-Waller Factor of MgO Powder by Elastic Neutron Scattering

(M.M. Beg)

The Debye-Waller exponent,  $B$ , for a powdered sample of MgO was determined at room temperature by elastic neutron scattering using a triple-axis spectrometer. MgO has the NaCl structure ( $a = 0.353 \text{ \AA}$ ), and the scattering lengths for Mg and O are almost equal. This causes the structure factors for reflections with Miller indices all odd to be  $\sim 500$  times smaller than the structure factors for reflections with Miller indices all even. Therefore, the all odd index Bragg reflections are forbidden for all practical purposes.

The Debye temperature,  $\theta_D$ , of MgO was determined previously by specific heat methods and different values were quoted for powdered and single crystal samples<sup>45)</sup>. It proved impossible to correlate the values for the powder sample and the single crystal by taking the sample particle size<sup>45)</sup> into account. The Debye temperature for MgO was also evaluated in the harmonic approximation from the phonon frequency distribution by Sangster et al.<sup>46)</sup> giving a value of 761 K. The results obtained by neutron scattering tend to give lower values of  $\theta_D$  than those obtained from the specific heat measurements.

The present experiment was performed with incident neutrons of an energy of 58.4 meV and an analyser energy resolution of 0.3 meV. Bragg peaks up to (422) were measured. Detailed computer calculations were performed to calculate the thermal diffuse scattering (TDS) contribution to the elastic peak on the model described by Beg et al.<sup>47)</sup>. The TDS for MgO was found to be negligible and varied from 0.07% for the (200) to 0.20% for the (420) peak. In a structure refinement, very good agreement was achieved between the calculated and observed structure factors with  $B = (0.354 \pm 0.008) \text{ \AA}^2$ . This corresponds to a Debye temperature of  $(743 \pm 8) \text{ K}$ . This result agrees with  $\theta_D = (754 \pm 7) \text{ K}$  obtained from specific heat measurements on a single crystal, especially since neutron scattering experiments tend to give low values for  $\theta_D$ , and the powdered nature of the sample tends to lower  $\theta_D$  by  $\sim 1/3 \%$ <sup>45)</sup>.

---

<sup>45)</sup> T.H.K. Barron, W.T. Berg, and J.A. Morrison, Proc. Roy. Soc. A250, 70 (1959).

<sup>46)</sup> M.C.L. Sangster, G. Peckham, and D.H. Saunderson, J. Phys. C. 3, 1026 (1970).

<sup>47)</sup> M.M. Beg, J. Aslam, Q.H. Khan, N.M. Butt, and S. Rolandson, Acta Cryst. A30, 662 (1974).

Neutron Slowing-Down by Bragg Reflection  
from a Moving Single Crystal

(S. Steenstrup (Physics Laboratory II, University of Copenhagen)  
and B. Buras)

The Monte Carlo calculations of neutron slowing-down by Bragg reflection from a moving single crystal<sup>48)</sup> were continued. The main results from the computer simulation experiment were:

- (1) Ultra-cold neutrons can in principle be produced from thermal neutrons by Bragg reflection from a moving single crystal. To achieve this, the velocity of the moving crystals (e.g. mica crystals) should be about half the velocity of the incident neutrons. Because there exists a technically feasible upper limit to the crystal velocity it is in practice necessary to start with cold neutrons (e.g.  $\sim 10 \text{ \AA}$  (or 400 m/s)).
- (2) The ultra-cold neutron flux (per unit solid angle and unit velocity interval) can be larger than the ultra-cold neutron flux extracted from the same neutron source even when the solid angle of the reflected beam is larger than that of the incident neutron beam.
- (3) The cross-section of the reflected ultra-cold-neutron beam is elliptical if the incident beam has axial symmetry. The minor axis of this ellipse is determined by the mosaic spread of the moving crystal and the major axis increases when the ratio between the velocity of the incident neutrons and the velocity of the reflected neutron increases.

---

<sup>48)</sup> B. Buras, K. Carneiro, S.E. Nielsen, E. Præstgaard, and  
S. Steenstrup, Risø Report No. 300, 46 (1973).

## 2. PLASMA PHYSICS

### Solid H<sub>2</sub> Film

(H. Sørensen)

The experimental arrangement<sup>49)</sup> for the study of interactions between charged particles and films of solid H<sub>2</sub> and D<sub>2</sub> has been used for preliminary measurements. A film is made by letting a molecular beam of cooled gas impinge on a target plate (12 mm diameter) held at 2.5-3 K. The growth rates are typically 10-1000 Å/s. The target plate is electrically insulated from the cryostat and it may thus be used to measure the beam current. The target plate is supplied with an electrical heater and a carbon resistance thermometer. It is then possible to remove a film quickly by heating the target to 12 K, and the target plate may be used as a calorimeter. The target may be biased electrically with respect to the grounded cryostat. A grid (at 12 K) in front of the target may be biased with respect to the target. In both cases the bias voltages are between -45 and +45 V.

The target plate can be irradiated by electrons ( $\leq 3$  keV) from an electron gun or light ions from a duoplasmatron ( $< 10$  keV). The beam may either be continuous or it may be a single pulse. Pulses as short as 0.7 ms have been used. At low particle energies it is difficult to get sufficiently high beam current, and practical lower limits for the energy (at present 300 eV for electrons and 2 keV for ions) are determined by the signal to noise ratios.

One would assume that solid D<sub>2</sub> is an electric insulator. However, when a thick D<sub>2</sub> film (thick with respect to particle range) is bombarded by a continuous ion beam, the beam current is transmitted through the film electrically. The current is independent of the target bias and equals the current measured when using the target plate as a calorimeter. This means that charge

---

<sup>49)</sup> H. Sørensen, Risø Report No. 300, 46 (1973).



carriers must be mobile in solid  $D_2$  and that a thick film only emits very few charged secondary and reflected particles. When the film is removed a current pulse is seen. The pulse indicates that a frozen-in positive charge exists in an irradiated film. The frozen-in charge may still be observed 20 minutes after the irradiation.

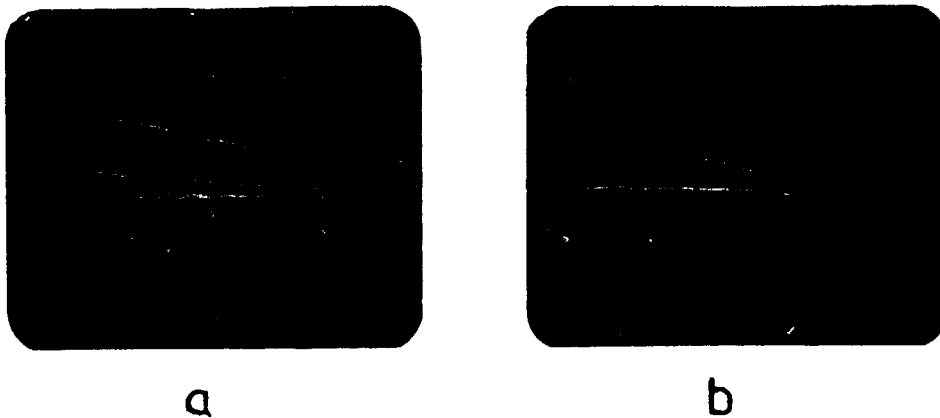


Fig. 16. Current flow from the target plate to ground observed when irradiating  $D_2$  films with 5 keV  $H_2^+$  pulses. a) Film thickness 1  $\mu m$ , 4 successive pulses. b) Film thickness 2  $\mu m$ , 2 successive pulses. Abscissa 2 ms/division, ordinate 50 nA/division. The grid is at +45 V with respect to the target.

Although the situation is different. For very short pulses the secondary electron current depends on the grid bias. The current rises with time and within some ms a saturation value is reached. The saturation value is equal to the value obtained for continuous irradiation and independent of the grid bias. The secondary electron current is emitted initially. As the positive ions are incident positive ions and the emitted secondary electrons, the outer part of the film charges up and retains the positive charge. The charge-up time depends on the current density and the film thickness as seen in fig. 16. As long as the positive and secondary electrons are pulled away from the target film, and the initial current is thus the sum of the secondary electron current and the ion current. The secondary electron current is determined by the secondary electron emission determined by the incident ion current.

When a film is bombarded with electrons the situation is similar. The film charges up and a frozen-in negative charge may be seen. The situation is, however, more complicated than for ion-irradiation and it is not yet understood.

The experiment offers several other possibilities. The lifetime of frozen-in charges could give information on mobilities of charge carriers and the ranges of electrons and ions in solid  $H_2$  and  $D_2$  could be studied. We observed that a very thin film is etched away by a beam. By utilising this one could investigate beam-desorption from different substrates. The preliminary measurements have shown that very little beam energy is back-scattered when solid  $D_2$  is irradiated with protons. One can then measure the energy back-scattered from a heavy target surface calorimetrically since the experiment permits a quick change of target surface.

#### Pellet Refuelling Problem. I: Theoretical Aspects (C.T. Chang)

In view of the low energy transport rate across the field lines and the anticipated low conductivity of the ablated plasma, we questioned the existence of a  $\beta = 1$  envelope around the pellet (the balloon model). Instead, the envelope was replaced by a flexible magnetic nozzle. The shape of the nozzle is determined by assuming that its boundary is an isobaric surface. The ablation rate of the pellet is then determined by assuming a sonic flow at the same pressure as that of the ambient medium at the exit of the nozzle. The ablation rate is seen to vary slightly with a field trapping parameter. Contrary to the prediction of the balloon model, it is shown that because of reduction of the gas pressure, an increase of the trapped field tends to reduce the ablation rate.

### Pellet-Fermelling Problem. II: Acceleration

(L. Hanch (Columbia University, U.S.A.), V.O. Jensen, L.W. Ingemann, H.H. Pécori, H. Sørensen, F. Øster, and Hans-Jørgen Winckler (Engineering Department))

A study group was formed to analyse the acceleration problem. Two values of the pellet velocity were considered, namely  $10^4$  m/s and 300 m/s. A pellet velocity of  $10^4$  m/s is suitable for the use of a reactor, whereas 300 m/s is believed to be a reasonable velocity at which to perform realistic ablation experiments in the near future. Previous acceleration proposals were (1) mechanical, (2) induction, (3) electrostatic, and (4) laser acceleration. Of these methods only electrostatic acceleration was found feasible to reach a pellet velocity of 300 m/s in practice.

We propose pneumatic acceleration using  $H_2$  at high pressure as the driving element. The high pressure is either supplied separately or by evaporation of a part of the pellet. In the latter case a part of the pellet should provide the evaporation and thus avoid any heating of the driving gas. The method may be used to reach a velocity of  $10^4$  m/s. A preliminary test at room temperature with pellets made of beeswax (density 10 times the density of  $H_2$ ) resulted in a pellet velocity of 100 m/s at a low value of the energy supplied to the spark.

### Energy Spectra Measurements. II: Charge Exchange Neutrals

(L.W. Ingemann and A.H. Højlund)

Neutral energy spectra of charge exchange neutrals have been measured using the neutral particle detector, and the ion energy distribution function has been calculated by a simple model for the retarding plasma. After integrating this distribution function over the energy range of the detector it was possible to compare the results with the measured energy spectra.

We found acceptable agreement with the theory. Later, when a calibration of the detector sensitivity at low energies has been made it may be possible to compare the energy spectra with a more detailed theoretical model.

#### Rotating Plasma Measurements. II: Doppler Broadening

(D. Dimock (Princeton University, U.S.A.), L.W. Jørgensen, and A.H. Sillesen)

The Doppler Broadening of a HeII (4686 Å) line was measured in a He plasma. The results agreed well with those obtained from the measurements on charge exchange neutrals.

#### Rotating Plasma Measurements. III: Electron Temperature

(D. Dimock (Princeton University, U.S.A.), M. Platina<sup>\*</sup>, M. Popović<sup>\*</sup> (<sup>\*</sup>Institute of Physics, Beograd), and A.H. Sillesen)

An attempt was made to measure the electron temperature in a H plasma by measuring the population of the excited states of the neutral H atoms. An absolute calibration of the monochromators was made using radiation from a W ribbon standard lamp. The radiation emitted parallel to the magnetic field of the first six lines of the Balmer series was measured. The temperature was found to be 0.3 eV. This is much lower than expected and suggests that the light does not come from the main part of the plasma but from the edges.

#### Pellet-Rotating Plasma Interaction. I: Pellet Velocity Measurement

(F. Øster)

The previous interaction experiments<sup>50)</sup> were performed with a fixed time delay between the launching of the pellet and the triggering of the rotating plasma. A new system has been devel-

---

<sup>50)</sup> L.W. Jørgensen, A.H. Sillesen, and F. Øster, *Risø Report* No. 300, 48 (1973).

oped. This system measures the velocity of each pellet and triggers the rotating plasma accordingly, i.e. when the pellet is at a preset position. The accuracy in positioning the pellet is improved from  $\pm 5$  cm to approximately  $\pm 1$  cm.

#### Pellet-Rotating Plasma Interaction. II: Spectroscopy

(D. Dimock (Princeton University, U.S.A.), M. Platiša\*, M. Popović\* (\*Institute of Physics, Beograd), A.H. Sillesen, and F. Øster)

Two monochromators were used to analyse the light emitted from the tail of the pellet created during the interaction with a He plasma. In principle, the light could have two origins, namely: (1) emission from pellet particles brought into their position in the tail by means of the  $\bar{E} \times \bar{B}$  drift, and (2) emission from plasma particles cooled by the interaction. One of the monochromators detected the HeII, 4686 Å line, and the other the H $\beta$ -line. The result of the measurements was that a somewhat higher intensity of the HeII line was observed with an interaction than without, but that the dominant light contribution in the tail originates from H particles from the pellet.

The set-up was also used to detect the velocity at which the pellet material appears in the tail. This experiment was performed both with H and He plasmas. It turned out that the light emitting particles are brought into the tail at a rather low velocity compared to the rotational drift velocity.

#### Investigation of the Farley Instability in the Q-Machine

(N.D'Angelo, H.L. Pécseli, and P.I. Petersen)

The plasma is created by surface ionization on a 2 mm thick Ta wire shaped as a spiral. Hereby a radial electric field is created that causes the plasma to rotate as a solid column. The background neutral pressure (in our case A) is adjusted so the ion-neutral collision frequency is equal to the ion cyclotron frequency. The neutral gas acts then as a drag on the ions while

the electron motion is virtually unchanged. This causes the electrons to drift through the ions and gives rise to the Farley instability. The instability is observed and the variation of the threshold neutral pressure is investigated as a function of B-field. We found agreement between the theory and the experimental results. We also investigated the spectrum of the oscillations. In the range 100-500 kHz the amplitude spectrum is described by a  $f^{-\alpha}$  power law, where  $\alpha \sim 1.8-2.0$ . Expecting the spectrum of the Farley instability and of the type II irregularities to be identical at short wavelengths this result is in agreement with the predictions of Ott and Farley<sup>51)</sup>. (The type II irregularities in the equatorial electrojet are caused by an instability driven by the vertical density gradients.)

#### Kelvin Helmholtz Instability

(N. D'Angelo, V.O. Jensen, P. Michelsen, H.L. Pécseli, and P.O. Petersen)

One method to heat up a plasma to thermonuclear temperatures may be the use of a high energy neutral beam. When such a beam interacts with a plasma it may excite several instabilities. Most likely, one of these is the Kelvin Helmholtz instability caused by the velocity shear between the fast ion beam produced by the neutral beam by charge-exchange or ionization processes and the background plasma. An experiment simulating this situation was set up in the Q-machine. In the centre of the plasma column and parallel with it was placed a small charge-exchange tube. A cloud of neutral Cs in this tube produces a beam of slow ions in the fast drifting background plasma. This should produce a sufficiently high velocity shear to make the plasma unstable to the Kelvin Helmholtz instability, but no instability was observed. An explanation of this result may be that the charge-exchange tube forms a cylindrically shaped shadow in the plasma column which separates the slow ions from the fast ones, and causes only a weak or no interaction between the two ion groups. Another method to simulate this instability is under consideration.

---

<sup>51)</sup> E. Ott, and D.T. Farley, J. Geophys. Res. 79 (1), 2468 (1974).

### Electron Heating at the Cyclotron Resonance

(P. Michelsen and H.L. Pécseli)

The temperature of the electrons is an important parameter in many experiments, and it is therefore of interest to be able to vary this parameter. For this purpose a microwave oscillator with a frequency range from 8 to 12.4 GHz and a 1 W amplifier was purchased. The energy fed into the system, when the microwave frequency is in resonance with the electron cyclotron frequency, increases the perpendicular component of the electron velocity. Either because of collisions or because of gradients in the magnetic field, part of this energy can be transferred into the parallel motion. The coupling to the plasma was examined in two ways, first by using a microwave horn and a reflector, and secondly by using a microwave cavity resonator. The latter proved to be the most efficient method but in both cases it was possible to raise the electron temperature more than a factor of ten.

### Ion Beam Instability

(V.O. Jensen, P. Michelsen, H.L. Pécseli, and J.J. Rasmussen)

The new possibility to vary the electron temperature and the earlier developed method to produce a double-humped ion velocity distribution function<sup>52)</sup> have given ample opportunities to examine the ion beam instability. The instability is excited when a beam of ions streams through a background plasma which is a common situation in many laboratory plasmas. Preliminary results obtained by measuring the frequency spectrum of the density fluctuations indicate that the instability is excited when the electron temperature is increased an order of magnitude from 0.2 eV to 2 eV. The range of unstable frequencies is from 0 to 100-200 kHz and agrees with the range expected from theoretical considerations.

---

<sup>52)</sup> S.A. Andersen, V.O. Jensen, P. Michelsen, and P. Nielsen, Phys. Fluids 14, 728 (1971).

### 3. NUCLEAR PHYSICS

#### An Attempt to Form the $^{236}\text{U}$ Fission Isomer with Thermal Neutrons

(V. Andersen, C.J. Christensen, S. Bjørnholm\*, J. Borggreen\*,  
and N.J.S. Hansen\* (\*Niels Bohr Institute, Copenhagen))

The possible formation of the fission isomer of  $^{236}\text{U}$  by thermal neutron irradiation of  $^{235}\text{U}$  has been searched for. The experiment<sup>53)</sup> is designed to detect possible fission fragments arriving about 100 ns after the detection of a prompt U-X-ray conversion electron coincidence originating from a transition in the second well of  $^{236}\text{U}$  ((e,X prompt)-f delayed). All detectors have large solid angles ( $\epsilon_F \sim 0.5$ ,  $\epsilon_\beta \sim 1$ ,  $\epsilon_X = 3\%$ ) and the time resolutions are  $\sim 10$  ns. A (e-f) delayed coincidence measurement with electron energies from 10 to 100 keV gives an approximate value of  $8 \cdot 10^{-6}$  for the isomer to prompt fission ratio,  $\sigma_{if}/\sigma$ . In the ((e,X)-f) delayed coincidence measurement the electron energy spectra were searched for electron lines with the correct energy spacing between the  $L_{I,II}$  and the  $L_{III}$  conversion (electrons observed in coincidence with  $L_\beta$ - and  $L_\alpha$ - X-rays, respectively). The most likely candidate found was a complex corresponding to a  $\gamma$ -ray energy of 46.4 keV, which could be a  $4^+ + 2^+$  transition in the rotational band of the second well. The contents of this complex would indicate a value of approximately  $1 \cdot 10^{-5}$  for the isomer ratio, but statistics is so poor that it is judged barely significant. Further calculations are needed before a final upper limit can be stated.

---

<sup>53)</sup> V. Andersen and C.J. Christensen, *Risø Report No. 200*, 14 (1973).



#### 4. METEOROLOGY

##### Change of Terrain Roughness

(N.E. Busch, K. Hedegaard, L. Kristensen, N.W. Nielsen, and E.W. Peterson (Oregon State University))

Analysis of data from Risø's 120 m tower reveals that for certain wind directions distinct kinks appear in the vertical profiles of the horizontal mean wind profiles. The kinks, which for some wind directions are double kinks, are believed to relate to changes in the roughness of the upstream terrain<sup>54, 55</sup>). Recent investigations<sup>56</sup>) indicate that mesoscale effects, and effects caused by topographically-induced pressure gradients, may have a more profound influence on the shape of the profiles than first believed.

The analysis of the data from the 120 m tower continues, but in order to investigate in more detail the change-of-terrain-roughness problem, three instrumented 13 m masts were erected along a line perpendicular to the north shore of the Risø peninsula. One tower is located on the beach, the two others approximately 53 and 177 m from the shore line. Each of the three masts is instrumented with six cup anemometers, two shielded thermometers, and one wind direction indicator. Turbulence intensities are measured at two heights (1 and 13 m). The towers are kept in continuous operation. The data are automatically compiled digitally on magnetic tape.

---

<sup>54</sup>) E.A. Taylor and E.W. Petersen, Quart. J. Roy. Meteorol. Soc. 11, 405 (1971).

<sup>55</sup>) E.W. Petersen and E.A. Taylor, Quart. J. Roy. Meteorol. Soc. 11, 411 (1971).

<sup>56</sup>) E.W. Petersen, to be published in Quart. J. Roy. Meteorol. Soc.

Preliminary analysis of data from the towers taken during periods with on-shore winds and near-neutral stability shows that the wind profiles adjust to the rougher land surface through wind profiles with inflection points, and that the air in the upper part of the internal boundary layer is accelerated to wind speeds which significantly exceed those corresponding to the unperturbed flow over the water at the same height. The latter effect is most probably caused by a low bluff on the beach.

### Atmospheric Gravity Waves

(E.L. Petersen)

A theoretical study of the generation and propagation of atmospheric gravity waves with special emphasis on wave-turbulence interaction is being undertaken. A simple "tank" model in which a discontinuity separates two adiabatic layers showed<sup>57)</sup> how a turbulent layer at the bottom can generate internal gravity waves. The amplitudes of the waves grow linearly or exponentially with time if the turbulence and the waves are assumed to be non-coupled or coupled, respectively. In both cases it was shown that there exists a resonance condition which favours the growth of waves in certain directions.

More generally it has been shown that from the linearized, inviscid, adiabatic, non-rotating, steady state theory it is feasible to estimate quantitatively the transport of energy and momentum deficit from a turbulent boundary layer owing to gravity waves.

A special study of atmospheric wave motion is performed on data from the National Center for Atmospheric Research-Continental Airlines Clear Air Turbulence Experiment 1973-74. The data currently being analysed consist of the horizontal components of the wind measured at 10 km altitude during 50 flights Chicago-Los Angeles-Honolulu by B-747 aircraft (fig. 17).

---

<sup>57)</sup> E.L. Petersen, in notes on the 1973 Summer Study Program in Geophysical Fluid Dynamics at The Woods Hole Oceanographic Institution. No. 73-41, 70 (1973).

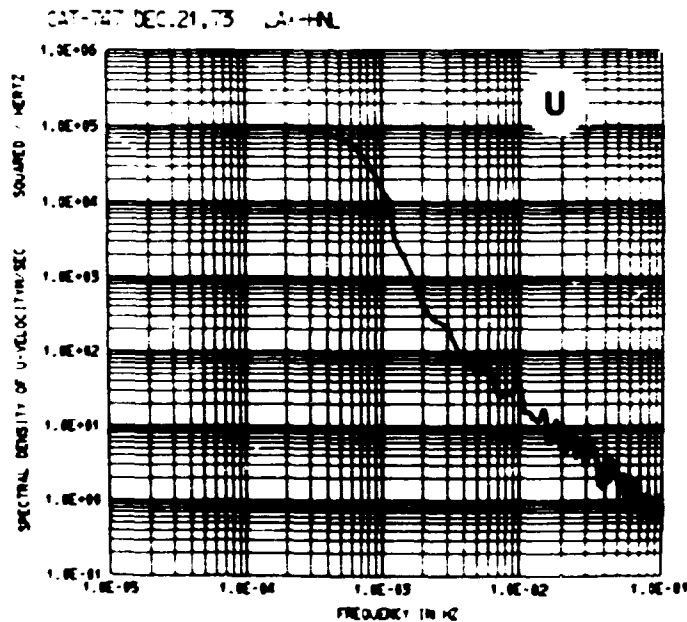
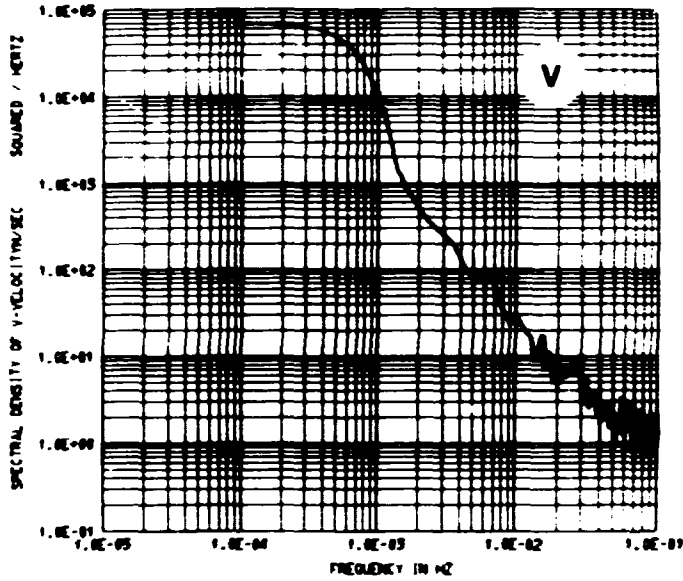


Fig. 17. Spectra of the horizontal wind components (u: east-west; v: north-south) as measured at an altitude of 10 km by an instrumented B-747 during flight from Los Angeles to Honolulu. The speed of flight was approximately 200 m/sec, so the spectra are almost true wavenumber-spectra with  $10^{-1}$  Hz corresponding to a wavelength of 2 km and  $10^{-4}$  Hz to 2000 km. The energy in the low frequency end is underestimated because of the methods of analysis.

### Simulation of Atmospheric Turbulence

(E.L. Petersen and J.A. Dutton (Pennsylvania State University, U.S.A.))

A method that produces realistic simulations of atmospheric turbulence has been developed and analysed. The procedure makes use of a generalized spectral analysis, often called a proper orthogonal decomposition or Karhunen-Loève expansion. A set of criteria is selected that emphasises a realistic appearance, a correct spectral shape, and non-Gaussian statistics in order to evaluate the model turbulence.

Turbulence records were analysed in detail providing both a background for comparison and input statistics for the generalized spectral analysis which in turn produced a set of orthonormal eigenfunctions and estimates of the distributions of the corresponding expansion coefficients. The simulation method utilizes the eigenfunction expansion procedure to produce preliminary time histories of the three velocity components simultaneously. As a final step a spectral shaping procedure is applied. The method is unique in modelling the three velocity components simultaneously, and it was found that important cross-statistical features behave reasonably well.

### Time Series Analysis

(S.E. Larsen, E.L. Petersen, and R.H. Jones (University of Hawaii, U.S.A.))

Procedures have been developed which estimate spectral characteristics of multivariate time series by means of fitting finite autoregressions to the data and calculating the spectra from the estimated regression coefficients and the one step prediction error variance. It is investigated how this type of spectral estimation compares with the usual estimation methods, i.e. either the smoothing of periodograms or the Fourier transformation of the correlation functions. The periodograms and the correlation functions are all calculated by use of a fast Fourier-transform algorithm which factors the dimension of the time series.

As a first step the order of the autoregression is identified by means of Akaike's information criterion<sup>58)</sup>. This order is mostly much smaller than the order to which the correlation functions are commonly calculated, i.e., one tenth of the dimension of the time series. It is found that the autoregressive spectra are much smoother than the corresponding spectra determined by Fourier transforming the correlation functions. However, if the two orders are chosen to be equal, the autoregressive spectra seem to show sharper peaks and valleys than found by the other spectral method.

The methods developed are currently being used in an attempt to detect climatic trends and fluctuations in data series obtained from ice cores from Greenland. These series, the Camp Century series and the Dye series, give indications of the temperature and precipitation thousands of years back.

#### Digital Noise

(L. Kristensen)

Whenever a stochastic time series is analysed digitally, the finite resolution  $D$  used to determine the signal will cause the estimates of the central moments to deviate systematically from those of the original signal. It has been shown<sup>59)</sup> that the estimated variance  $\sigma^2$  is equal to the true variance  $\sigma_0^2$  plus  $D^2/12$ . It is of particular interest to know how a signal, which is sampled digitally with a sampling period  $\Delta t$ , will have the additional variance  $D^2/12$  distributed on frequencies in a subsequent digital Fourier analysis. It seems obvious that the decisive question is how much the signal varies compared to  $D$  in the period  $\Delta t$ . A detailed analysis has shown the importance of a certain characteristic time scale, the Taylor microscale  $\lambda$  (fig. 18). If a gaussian process is considered, then  $\lambda$  is equal to the reciprocal of the average number of times the original signal crosses its mean value per unit time.

---

<sup>58)</sup> H. Akaike, Ann. Inst. Statist. Math. 23, 163 (1971).

<sup>59)</sup> W.F. Foyard, Proc. London Math. Soc. 29, 353 (1898).

The main result of the analysis is that the "digital noise"  $D^2/12$  is white<sup>60)</sup> if

$$\frac{\sigma_0}{D} \cdot \frac{\Delta t}{\lambda} > 1.$$

This condition and the relation  $\sigma^2 = \sigma_0^2 + D^2/12$  may serve as guidance, when  $D$  and  $\Delta t$  are to be chosen before digital recording. Correction for digital noise is easy, if the noise may be considered white.

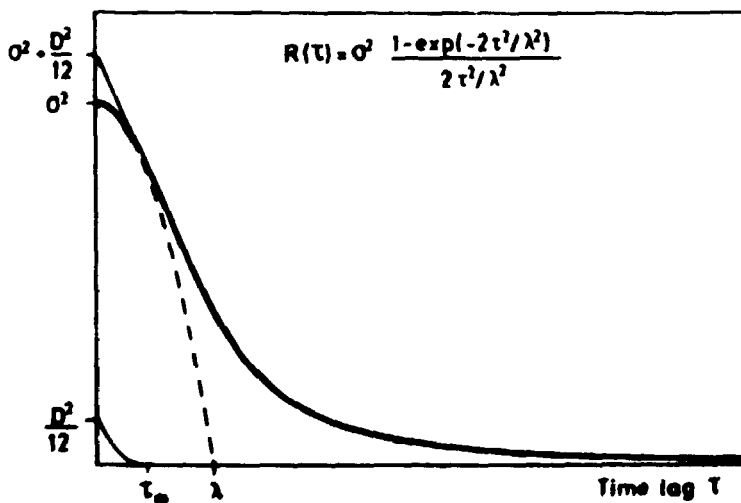


Fig. 18. The autocovariance function  $R(\tau)$  for a signal which is sampled with infinitely fine resolution and the autocovariance function  $R(\tau) + \Delta(\tau)$  for the same signal sampled with finite resolution  $D$ . The condition that a digital Fourier transformation with the time resolution  $\Delta t$  will transform  $\Delta(\tau)$  into a flat spectrum is that  $\Delta t$  is greater than the lag  $\tau_g$  at which  $\Delta(\tau)$  becomes zero. An analysis shows that  $\tau_g = 0.4 D\lambda/\sigma$ . Consequently, a sufficient condition that the digital noise is white is  $\Delta t > D\lambda/\sigma$ .

<sup>60)</sup> L. Kristensen, Risø-M-Report No. 1750 (1974).

### Air-Sea Interaction

(N.E. Busch and K. Hedegaard)

The analysis of profile data from the Kattegat-73 Experiment has been brought to an end. In that experiment a 40 m tower was erected in the Kattegat on 25 m of water and with a distance of about 20 nautical miles to the nearest shores. In the prevailing wind direction, the unobstructed fetch was 2 to 3 times longer.

The most important result of the analysis is that the drag coefficient  $C_D = (u_* / \bar{u})^2$  appears to be a simple function of the Reynolds number  $Re = u_* z_o / \nu$  independent of density stratification. Here  $u_*$  is the friction velocity,  $\bar{u}$  is the mean wind speed at a height of 10 m,  $z_o$  is the roughness length, and  $\nu$  is the kinematic viscosity of air. The power law relation between  $C_D$  and  $Re$  suggested by Kitaygorodsky et al.<sup>61)</sup> fits the Kattegat data excellently. The Kattegat experiments will be continued in the coming year in cooperation with the Institute of Physical Oceanography, University of Copenhagen, and the Geophysical Institute, University of Bergen.

### Fine Structure Experiment

(N.E. Busch, N.O. Jensen, L. Kristensen, S.E. Larsen, C.A. Paulsen<sup>†</sup>, P.M. Williams<sup>†</sup> (<sup>†</sup>Oregon State University, U.S.A.), N.E.J. Boston<sup>x</sup>, T.M. Houlihan<sup>x</sup> (<sup>x</sup>Naval Postgraduate School, Monterey, U.S.A.), F.E. Jerome (Malaspina College, British Columbia), F.H. Champagne<sup>\*</sup>, T. Leaton<sup>\*</sup>, C.H. Gibson<sup>\*</sup>, and J.A. Eriksen<sup>\*</sup> (<sup>\*</sup>University of California, San Diego, U.S.A.))

The behaviour of the small-scale turbulent fluctuations of various atmospheric parameters is of considerable interest from both scientific and technological points of view<sup>62)</sup>. Uncertainties exist especially concerning the small-scale behaviour of the

---

<sup>61)</sup> V.A. Kitaygorodsky, V.A. Luninsov, and G.N. Panin, Izv., Atmos. and Ocean. Phys. 9, 1135 (1973).

<sup>62)</sup> N.H. French, R.F. Bean, Y. Furukawa, G.A. McBean, and G. Strickland, Boundary-Layer Meteorol. 5, 211 (1973).

temperature fluctuations. The discussions mostly concentrate on the conditions for the existence of an inertial subrange in the temperature spectrum and on the appropriate value of the corresponding Kolmogorov constant. In order to study these problems, an experiment was carried out along the Risø tower in November 1973. Based on experiences gained from this experiment, a larger but similar experiment was conducted in August and September 1974.

The measurements were carried out to give information about the three-dimensional velocity field and the temperature field over time scales ranging from one hour to 0.2 minute along the whole (120 m) tower. This enables one to evaluate the tendency towards local isotropy for the velocity field and the temperature field at several heights at the same time, and to analyse the behaviour of the small-scale structure over almost two decades of Reynolds numbers.

The instrumentation and experimental procedure can be briefly described as follows: temperature and velocity profiles were measured by means of the standard instrumentation on the tower. Three three-dimensional ultrasonic anemometer-thermometers and one three-dimensional hot-wire probe plus a cold-wire probe were used to measure the turbulence velocity and temperature field at four heights. The fine-structure temperature fluctuations and horizontal velocity fluctuations were measured at seven heights by means of straight vertical hot-wires and cold-wires. The cold-wire diameters ranged from 0.25 to 1  $\mu\text{m}$ . All data were recorded directly on digital tape with a digitizing rate of 200 Hz except for the sonic and the profile data which were sampled once every 0.05 second and 10 minutes, respectively. The fine-structure data were differentiated and both the direct and the differentiated signals were recorded on analog tape for later fast digitizing.

Although one could have wished for a higher temperature fluctuation level, the on-line analysis showed that the data obtained seem to be of high quality. The further analysis is planned to take place in the various laboratories, and sequences are being selected for detailed analysis.



In connection with the experiment various technical development projects were undertaken. A number of differentiators were designed and built. They have Bessel-filter transfer functions to ensure a linear phase-transfer. The design permits independent setting of gain, zero-dB frequency (0.1-100 Hz), and lowpass cut-off (0.5-10 kHz). In cooperation with the Laboratory of Acoustics at the Technical University of Denmark, a method was developed which allows determination of the time-response of cold-wires by means of sinusoidal air temperature variations generated by a strong sound field variable from 0.020 to 10 kHz.

### Climatology in Greenland

(N.E. Busch, G. Jensen, L. Kristensen, and J. Taagholt  
(Ionosphere Laboratory, Danish Meteorological Institute))

Together with the Danish Meteorological Institute, and with help from The Royal Danish Air Force, The Sirius Sledge Patrol, and Eigil Knuth, the Meteorology Section operates three unmanned climatological stations or Unmanned Geophysical Observatories in North Greenland. The first UGO was put into operation in June 1972 at Nord ( $81^{\circ}36' \text{ N}$ ,  $16^{\circ}40' \text{ W}$ ), when Station Nord was closed by a governmental decision. The second UGO was installed in June 1973 at Kap Harald Moltke ( $82^{\circ}09' \text{ N}$ ,  $29^{\circ}53' \text{ W}$ ), where since 1957 a wide clay plain has been used as an emergency landing strip. In connection with a military survey for a future unmanned airport in North Greenland, a third UGO was established in July 1974 on the north tip of Greenland (Kap Morris Jesup,  $83^{\circ}38' \text{ N}$ ,  $33^{\circ}12' \text{ W}$ ).

An UGO consists in its present version of a battery-driven datalogger and instruments which measure temperature, dew-point, soil temperature, pressure, wind direction, and wind speed. The measurements are recorded digitally once an hour on 1/4 inch magnetic tape which is recovered and brought back once a year<sup>63)</sup>.

---

<sup>63)</sup> L. Kristensen and J. Taagholt, Unmanned Geophysical Observatory at Nord in North Greenland, Danish Meteorological Institute, Copenhagen (1973).

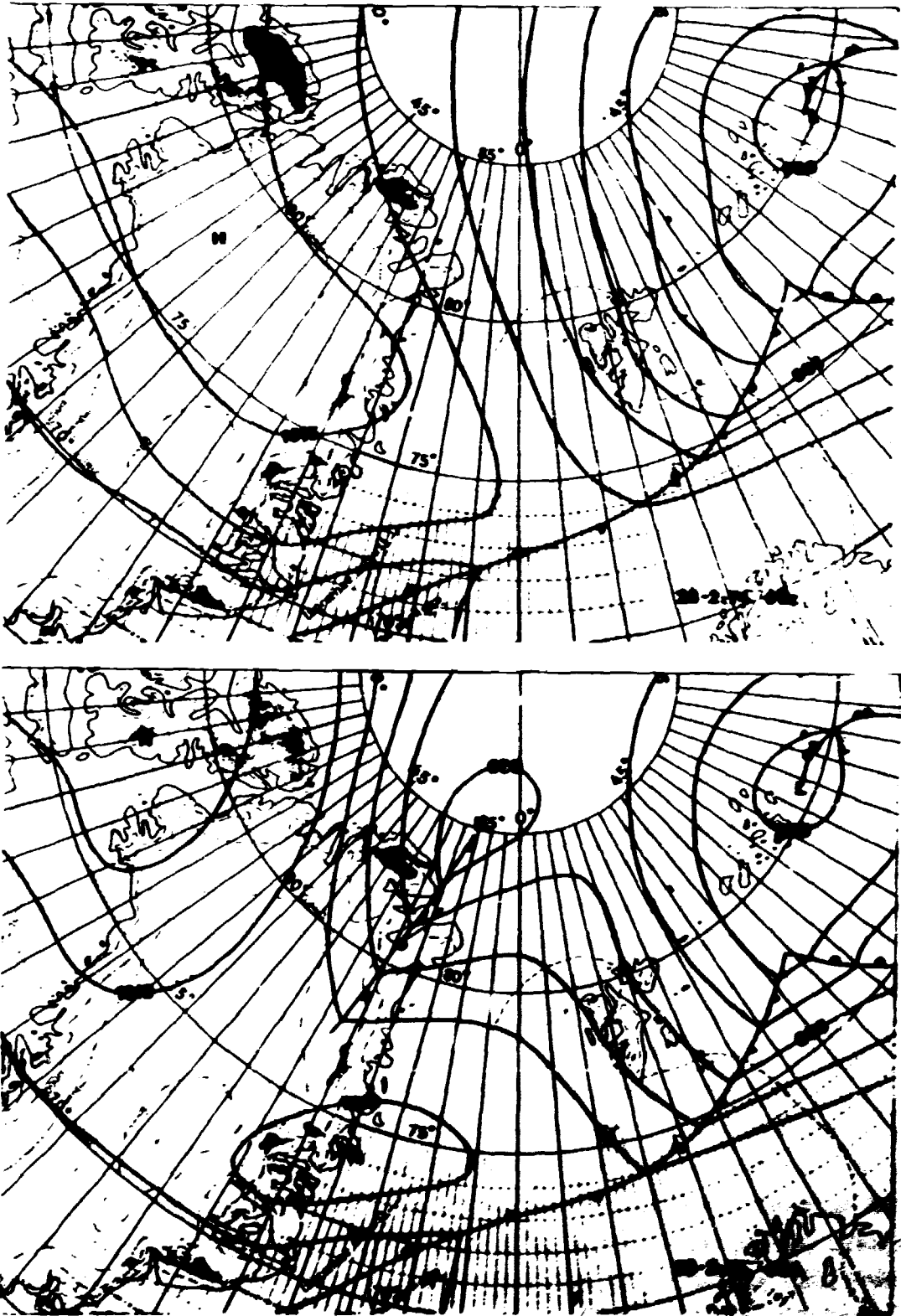


Fig. 19. Surface weather maps depend in some situations on particular pressure observations. This is illustrated in two maps from February 28, 1974, at 06 h<sup>00</sup> showing the features without (top) and with consideration of the pressure observations from UGO-Nord and UGO-North. The upper map is the result of the original analysis by the British Weather Service in which, for instance, the wave front along East Greenland is missing.

During its first year of operation UGO-Nord unfortunately stopped after approximately six months, probably because the datalogger's temperature control system in its original form was not efficient enough to cope with the cold environment<sup>64)</sup>. Data from the period 1973 to 1974 show that UGO-Nord as well as UGO-Moltke have operated satisfactorily.

#### Numerical Modelling of the Planetary Boundary Layer

(N.E. Busch, N.O. Jensen, R.A. Anthes<sup>+</sup>, and S. Chang<sup>+</sup>

<sup>+</sup>(Pennsylvania State University, U.S.A.))

The degree of accuracy and the detail of the planetary boundary layer (PBL) to be resolved in a dynamic model depend mainly on the characteristics of the phenomenon to be modelled. For example the short-range behaviour of the quasi-geostrophic waves in the westerlies may be modelled without any representation of the PBL at all. As long-term integrations of the general circulation or the behaviour of individual cyclones and smaller scale phenomena are considered, the PBL becomes more important. In some of these latter models, the detailed structure of the PBL is unimportant and only its net effect needs to be considered. In others, a more detailed representation of the PBL is necessary. One phenomenon that is strongly dependent not only on the gross effect of the PBL, but probably also on the details of the boundary layer structure, is the hurricane.

A simple model of the PBL is proposed which appears suitable for a more realistic simulation of the detailed structure of the hurricane boundary layer. Although designed with some of the hurricane problems in mind, the scheme is general and should be suitable for use in a wide variety of atmospheric models. The basic assumption in the model is that the diffusivity  $K$  for vertical exchange is related to the local friction velocity  $u_*$

---

<sup>64)</sup> N. Jensen, L. Kristensen, and J. Taagholt, Unmanned Geophysical Observatories in North Greenland 1972-1974, Danish Meteorological Institute, Copenhagen (1974).

and a mixing length  $\lambda$  through  $K = \lambda u_{*}$ , where  $\lambda$  obeys the prognostic equation

$$\frac{\partial \lambda}{\partial t} = \frac{\lambda_s - \lambda}{a \lambda / u_{*}}.$$

Here  $a$  is a constant and  $\lambda_s$  the mixing length pertaining to stationary situations. In the numerical work done so far we have used

$$\lambda_s = \frac{kz}{\phi_m} \left(1 - \frac{z}{h}\right),$$

where  $\phi_m$  is the non-dimensionalized wind-shear, and  $h$  is the height of the capping inversion. In a preliminary numerical experiment, the behaviour of the PBL agrees well with the observations of the Great Plains experiment.

#### Stress-Profile Experiment

(N.E. Busch, N.O. Jensen, and L. Kristensen)

One of the numerical models of the planetary boundary layer developed at Risø utilizes direct closure in terms of a modified K-theory which is formulated on the basis of long-term records of wind and temperature profiles along the Risø tower.

Since the estimation of momentum and heat fluxes from profile measurements was based on surface layer concepts which strictly speaking require horizontal homogeneity, a direct test of the applicability of the method was appropriate. To this end three 3D-ultrasonic anemometer-thermometers were operated at different levels along the Risø tower simultaneously with the ordinary routine instrumentation. Through twenty-four hours a 25 minute record was made once an hour. All the sonic signals were sampled at a rate of 100 samples per second. The synoptic situation was very steady. A high pressure ridge over the North Sea moved very slowly towards the east. The data are therefore not masked by large scale synoptic disturbances, but show structural changes as a result of the diurnal cycle. The data are undergoing detailed analysis.

## Wind Power

(N.O. Jensen)

Under the impact of the oil crisis and the debate concerning alternatives to our traditional energy sources, the magnitude and variability of wind power were subjected to an investigation<sup>(55)</sup>.

The theory for wind machines shows that the output is proportional to the third power of the wind-speed and proportional to the areas swept by the machine. In practice, however, there will be a wind speed below which the machine cannot operate as well as an upper wind speed above which the efficiency will drop drastically. On the basis of experience from full-scale electricity-producing wind machines, the following model was adopted: lower limit 4 m/s, upper limit 15 m/s, and aerodynamic efficiency 50% in this interval. Wind speeds greater than 15 m/s only make a contribution to power production that corresponds to 15 m/s. Estimates

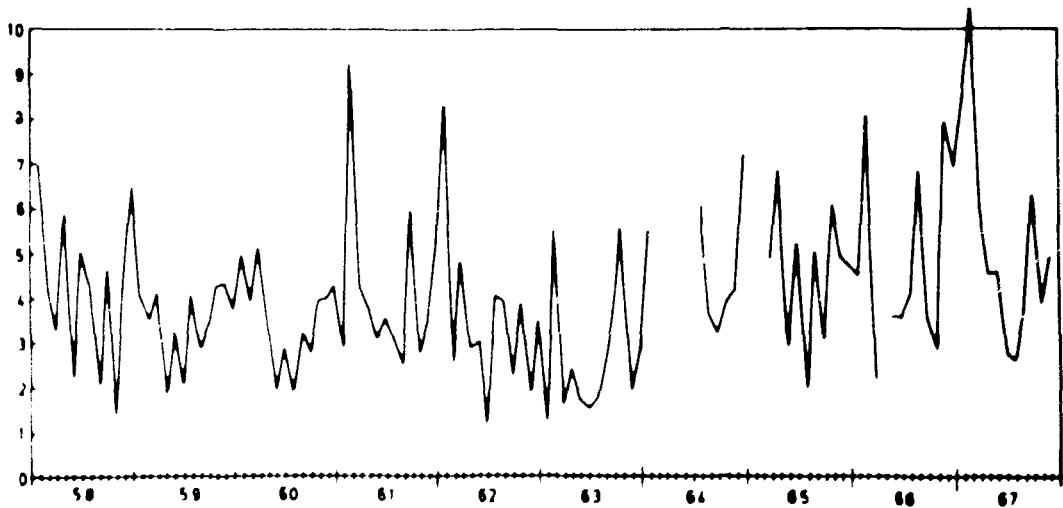


Fig. 20. Calculated production in MWh/month for a 10 m diameter wind turbine placed at a height of 23 m for the period 1/1-1958 to 31/12-1967. (10 MWh/month corresponds to an average production rate of 14 kW).

of the production of electric power by a wind turbine placed in various heights above terrain were obtained by use of the wind-speed data from the Risø tower for a period of ten years. Some results are shown in fig. 20.

### Dynamic Wind Loading

(N.E. Busch, O. Christensen, and S.E. Larsen)

In 1970 a wind-load committee was established by the Danish Engineering Association (Dansk Ingeniørforening) and authorized to revise the Danish Wind-Load Code. The present code was introduced in 1945 and supplemented in 1955 because of failures of certain types of roofs. Chapters on dynamic wind loading were not included in the code. In 1966, however, a preliminary wind-load code was published in which the concept of gust factors for slender structures of low damping was introduced. The theory was developed by A.G. Davenport<sup>66</sup>).

The dynamic part of the wind code was of particular interest to us. Our proposal for the code is based on Davenport's approach, that is on the concept of equivalent static load. A gust factor  $\phi$  is determined by which the mean-wind force on the structure is multiplied in order to obtain the design load. The gust factor  $\phi$  is given by

$$\phi = 1 + RP\sqrt{T_b + T_r} ,$$

where R is a roughness factor proportional to the turbulence intensity at the top of the structure, and P is a peak-factor incorporating the extreme-value distribution of the deflections of the top of the structure. The one-dimensional energy spectrum pertaining to the longitudinal turbulent velocity component in the undisturbed flow field is used to characterize the fluctuating forces which force the structure to respond dynamically. The response is assumed to be linear. The background stimulation

---

<sup>66</sup>A.G. Davenport, J. Structural Div., ASCE, 92, No. St3, 11 (1967).

$T_L$  is the contribution to the variance of the structural deflections under the assumption of critical damping of the structure. The symbol  $T_v$  represents the contribution to the deflection variance from the turbulent energy in resonance with the structure.

The structure response can be modelled as a system of three linear filters in series. Two of the filters are of first order and transmit the turbulent kinetic energy to the structure as pressure forces. The cut-off frequencies are determined by the linear dimension of the structure. The third filter is actually two filters in parallel: one ideal band-pass filter at the natural frequency of the structure and one second-order filter with cut-off frequency equal to the natural frequency.

The committee feels that it is very important that the revised code appear in a form which is both easy to use and scientifically sound. Therefore, the committee is considering a new basis for the specification of design wind velocities in Denmark, namely 1 minute average and extreme friction velocities. The design wind profile may be written

$$\frac{\bar{v}_z}{u_*} = 0.4 P' \ln \frac{z}{z_0},$$

where  $z$  is height above ground,  $z_0$  is the roughness length, and  $u_*$  is the friction velocity. The factor  $P'$  is a peak factor which takes into account the extreme-value statistics, and  $\bar{u}$  is the wind speed averaged over 10 minutes.

As a first step, the revised code will be published in 1974.

#### Applied Meteorology in Site Evaluations

(Chr. Jensen, Niels Jensen, E. Kristensen, and G.E. Larsen)

The committee is engaged in the site evaluation and safety studies preceding the first nuclear power plants in Denmark. The work is directed towards the information necessary to describe reactor

sites from the point of view of atmospheric dispersion. The section operates three automatic meteorological stations close to possible future reactor sites in order to obtain local statistics on meteorological parameters relevant to dispersal calculations. On the basis of data accumulated along the Risø tower, the section is currently studying Pasquill-class statistics, both when the Pasquill-classes are obtained from the standard deviation of wind direction fluctuations and when they are obtained from the vertical temperature gradients in the lowest 100 m of the atmospheric boundary layer as proposed in Safety Guide 23 (USAEC, 1972).

#### Applied Meteorology. II: Air Pollution Studies

(N.E. Busch, N.O. Jensen, L. Kristensen, and S.E. Larsen)

Within the field of general air pollution studies, the section cooperates with a number of scientific and technological groups on various projects.

In support of a study undertaken by Dansk Kedelforening (Danish Boiler Association) of air quality in the vicinity of a large power plant, a 40 m meteorology tower was erected at Stignæs in the southwestern part of Sealand. The tower is instrumented with wind and temperature sensors at several heights. This project was finished by the end of 1973 and the data compiled and organized during 1974. However, the meteorological measurements continue, partly in order to enlarge the climatological data series already collected, partly in support of the COST-62a project.

In the COST-62a project the chemistry and dispersion of various airborne pollutants from a power plant in southwestern Sealand (Stignæs) are investigated. The project is carried out as a tracer experiment by the Aerosol Laboratory at Risø. The plume is followed and studied by means of an instrumented aircraft. The meteorology section supplies the meteorological information.



necessary for the project such as dispersion calculations and reports before the flights, the latter with assistance from the Danish Meteorological Institute.

In connection with another air-pollution project carried out by Dansk Meteorologisk Institut in Fredericia, the section supplies meteorological measurements from a 43 m tower. Here wind speed and direction are measured at 10 and 42 m, while temperatures are measured at the 1.8 and 34.8 m levels.

In connection with an investigation carried out by Storkøbenhavn Luftrengøringsskud (Greater Copenhagen Air Pollution Committee) on air pollution in Copenhagen, the meteorology section is currently running two automatic meteorological stations, one in central Copenhagen (Margretheholmen) and one in the western outskirts (Herstedvester). At both stations wind speed and direction are measured at a height of approximately 10 m, while temperatures are measured at 2 m and 40 m above terrain.

#### Air Pollution Statistics

Co-ordinator: H.L. Petersen, C. Hennrichsen, (IMSOR, The Technical University of Denmark), and L. Mage (USEPA, Las Vegas, U.S.A.)

As yet, little is known about the statistical characteristics of a given pollutant and their relation to the averaging times for which the pollutant is wanted but not measured through a set of empirical statistical laws<sup>(1)</sup>. The laws are based on the assumptions that the pollutant is log-normally distributed for all averaging times and that a power law relation exists between the median value and the averaging time. These laws were originally proposed on the basis of statistical analyses of pollutant time series. These and other analyses published by various authors show, however, that the agreement between the laws and the data ranges from excellent to substantially less than fair. This fact combined with the purely empirical derivation makes a validation of their use extremely difficult.

<sup>(1)</sup>See, for example, A. G. Wilson, *Atmospheric Pollution*, 14 (1969).

To improve this situation a theoretical analysis was undertaken that has brought the laws within the framework of standard statistical analysis. In the course of this analysis, it was shown that the problem can be advantageously attacked in terms of the relation between sample variance, averaging time, and correlation functions or power spectra<sup>68)</sup> (fig. 21). It was also shown that the theoretical as well as practical advantages connected with the use of a three-parameter log-normal rather than the basic two-parameter log-normal distribution may outweigh the disadvantages associated with the addition of an extra parameter<sup>69)</sup>.

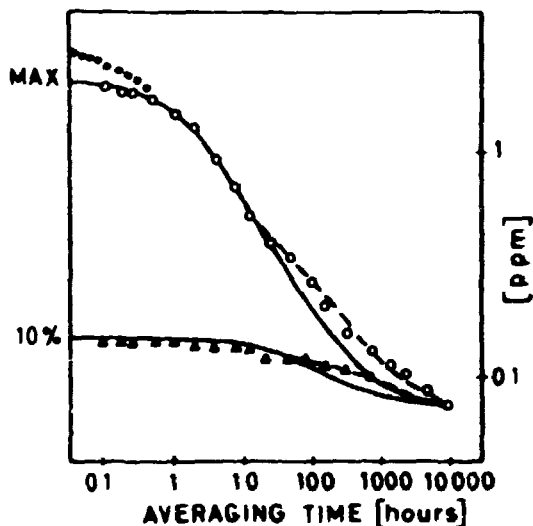


Fig. 21. The maximum values and the 10% percentiles versus averaging time for  $\text{NO}_x$  data from Washington DC. O and  $\Delta$  are the measured values taken from<sup>67)</sup>. —: Calculated curves assuming an exponential autocorrelation function. ---: Calculated curves assuming the autocorrelation function to be the sum of two exponential functions. ···: Calculated curve neglecting the time constant of the instrument<sup>67)</sup>.

## 5. LIQUID $\text{N}_2$ AND He PLANT

The production of liquid  $\text{N}_2$  and He amounted to 200000 and 10460 litres respectively. Out of these amounts, 5396 litres of liquid He were delivered to laboratories in Copenhagen and Århus.

<sup>68)</sup> S.E. Larsen and E.L. Petersen, Proceedings of the Symposium on Atmospheric Diffusion and Air Pollution, Santa Barbara 1974, 163 (AMS, Boston, 1974).

<sup>69)</sup> D.T. Mage, Proceedings of the 5th Meeting Expert Panel on Air Pollution Modeling, Risø 1974, NATO/CCMS, Bruxelles, 29.1 (1974).

## 6. EDUCATIONAL ACTIVITIES AND PUBLICATIONS

### Lectures

J. Als-Nielsen, Ferromagnetism in the Dipolar Coupled Ising System  $\text{LiTbF}_4$ :

- 1) Bell Laboratories, Murray Hill, New Jersey (September 1974).
- 2) Cornell University, Ithaca, New York (September 1974).
- 3) Harvard University, Boston, Massachusetts (September 1974).
- 4) M.I.T., Cambridge, Massachusetts (September 1974).
- 5) H.C. Ørsted Institute, Copenhagen (October 1974).

J. Als-Nielsen, Fernelysik (50 lectures in nuclear physics).  
Technical University of Denmark.

E. Fjell, Elastic Scattering of Neutrons by Phonons  
(6 lectures and subsequent neutron scattering experiments).  
University of Copenhagen and Risø.

E. Fjell, Neutron Diffraction Studies under High Pressure:  
1) University of Umeå, Sweden (February 1974).  
2) Studsvik, AB Atomenergi, Sweden (February 1974).  
3) Eidgenösscher Institut für Kernforschung,  
Würenlingen, Switzerland (March 1974).

E. Fjell, Nuclear Methods in Solid State Physics:  
Scattering of Neutrons in Solids (lecture series).  
University of Copenhagen.

M.H. Funch, Atmospheric Boundary-Layer Models.  
The University, Blindern, Oslo, Norway (May 1974).

M.H. Funch, Atmospheric Boundary-Layer Research at Risø.  
a) Florida National Laboratory, Tennessee (April 1974).

M.H. Funch, Meteorological Research at Risø. The Pennsylvania  
State University, Pennsylvania (April 1974).

K. Carneiro, The Dynamics of Simple Liquids Studied by Neutron Scattering:

- 1) University of Kent, Canterbury, England (May 1974).
- 2) Université de Paris VI, Orsay, France (May 1974).
- 3) Laboratório de Física e Engenharia Nucleares, Sacavem, Portugal (May 1974).
- 4) Chalk River Nuclear Laboratories, Chalk River, Canada (September 1974).

K. Carneiro, Phonons in Solid and Liquid Hydrogen Studied by Inelastic Neutron Scattering. Technical University of Denmark (April 1974).

C.T. Chang, On the Magnetic Shielding Effect of a Refuelling Pellet:

- 1) Institute of Plasma Physics, Royal Institute of Technology, Stockholm, Sweden (July 1974).
- 2) Culham Laboratory, Abingdon, England (December 1974).

O.W. Dietrich, Courses in Physics, Roskilde Universitets Center.

O.W. Dietrich, EuO and EuS - Nature's Best Examples of Heisenberg Ferromagnets. Kernforschungsanlage, Jülich, Germany (June 1974).

J.G. Houmann, Magnetic Excitations in Praseodymium Studied by Inelastic Neutron Scattering:

- 1) Oak Ridge National Laboratory, Tennessee (December 1974).
- 2) Brookhaven National Laboratory, New York (December 1974).

N.O. Jensen (3 double lectures). Technical University of Denmark (October 1974):

- 1) Meteorology og Aerodynamik i Relation til Luftforurening. ("Meteorology and Aerodynamics in Relation to Air Pollution").
- 2) Atmosfæriske Spredningsmekanismer og Modeller. ("Atmospheric Diffusion Mechanisms").
- 3) Røgfanemodeller, Anvendelser og Begrænsninger. ("Plume Dispersion Models, Applications and Limitations").

V.O. Jensen, Fusionsenergien, kommer den og hvornår? ("Fusion Energy - if and when?") Danish Engineering Society, Copenhagen (October 1974).

- V.B. Jensen, Fusion Research, Status and Prospectives.  
Institute of Physics, University of Aarhus (May 1974).
- V.B. Jensen, Plasmatysik (50 lectures in Plasma Physics).  
Technical University of Denmark.
- J.K. Kjems, Dynamics of the Cooperative Jahn-Teller Transition  
in  $\text{FeAlO}_3$ :  
1) Chalk River Nuclear Laboratories, Ontario, Canada  
(January 1974).  
2) Iowa State University, Ames, Iowa (May 1974).  
3) Argonne National Laboratory, Illinois (May 1974).  
4) Oak Ridge National Laboratory, Tennessee (May 1974).
- J.K. Kjems, Neutron Scattering from  $\text{N}_2$  in Two and Three  
Dimensions. University of California, Los Angeles,  
California (September 1974).
- H.-A. Linigini, Hahn-Meitner-Institut für Kernforschung,  
Berlin, Germany (December 1974):  
1) Phase Transition with Two Order Parameters  
Exemplified by Rare Earth Alloys.  
2) Spin Waves and Magnetic Properties of the Nearly  
Two-Dimensional Antiferromagnet  $\text{NiCl}_2$ .
- M. Nielsen and K. Carneiro, University of Odense (April 1974):  
1) Neutron Scattering as an Experimental Tool.  
2) Phonons in Solid and Liquid Hydrogen Studied by  
Inelastic Neutron Scattering.
- Rolf M. Lenz, Thermal Fluctuations and Turbulence in Plasma.  
Danish Space Research Institute, Lyngby (February 1974).
- E.L. Peterson, Excitation of Internal Gravity Waves by a  
Continuous Boundary Layer:  
1) Pennsylvania State University, State College,  
Pennsylvania (January 1974).  
2) Wave Propagation Laboratory, National Oceanic  
and Atmospheric Administration, Boulder,  
Colorado (August 1974).

E. Warming, Solid State Work in the Scattering Group at Risø.  
Joint Institute of Nuclear Research, Dubna, U.S.S.R.  
(October 1974).

Flemming Øster, The Ablation Rate of Hydrogen Pellets in Hydrogen  
and Helium Plasmas. Kharkov Physical Technical Institute,  
U.S.S.R. (April 1974).

### Publications

J. Als-Nielsen, L.M. Holmes, and H.J. Guggenheim, Wave Vector  
Dependent Susceptibility at  $T > T_c$  in a Dipolar Ising  
Ferromagnet. Phys. Rev. Lett. 32 (1974) 610-613.

V. Andersen, Solid Angle for Electron Detection in a Homo-  
geneous Magnetic Field. Nucl. Instr. and Meth. 122 (1974)  
543-545.

P. Bak, Excitations and Magnetic Properties of Rare-Earth  $Al_2$   
Compounds. Risø Report No. 312 (1974) 62 pp.

P. Bak, Magnetic Properties of  $NdAl_2$ .  
J. Phys. C 7 (1974) 4097-4103.

R.J. Birgeneau, J.K. Kjems, G. Shirane, and L.G. van Uitert,  
Cooperative Jahn-Teller Phase Transition in  $PrAlO_3$ .  
Phys. Rev. B 10 (1974) 2512-2534.

B. Bonnevier and A.H. Sillesen, Breakdown and Plasma Formation  
in a Rotating Plasma Device. Trita-EPP-74-06 (1974) 10 pp.

B. Buras and L. Gerward, Relations between Integrated Intensities  
in Crystal Diffraction Methods for X-Rays and Neutrons.  
Physical Laboratory II, H.C. Ørsted Institute, University  
of Copenhagen, Monograph No. 74-20 (1974) 18 pp. (Also  
Report No. 7, Laboratory of Applied Physics III,  
Technical University of Denmark).

- B. Buras, J. Staun Olsen, L. Gerward, B. Selsmark, and A. Lindegaard Andersen, Energy Dispersive Spectroscopic Method Applied to X-Ray Diffraction in Single Crystals. Physical Laboratory II, H.C. Ørsted Institute, University of Copenhagen, Monograph No. 74-21 (1974) 23 pp. (Also Report No. 8, Laboratory of Applied Physics III, Technical University of Denmark).
- B. Buras, J. Staun Olsen, A. Lindegaard Andersen, L. Gerward, and B. Selsmark, Evidence of Escape Peaks Caused by a Si(Li) Detector in Energy-Dispersive Diffraction Spectra. J. Appl. Cryst. 7 (1974) 296-297.
- K. da Costa Carneiro, The Dynamics of Liquid Hydrogen and Liquid Nitrogen Studied by Inelastic Scattering. Risø Report No. 308 (1974) 54 pp.
- K. Carneiro and M. Nielsen, Neutron Scattering in Solid and Liquid H<sub>2</sub>. In: Anharmonic Lattices, Structural Transitions, and Melting. Edited by T. Riste (Nordhoff, 1974).
- K. Carneiro, M. Nielsen, and J.P. McTague, Collective Excitations in Liquid Hydrogen Observed by Coherent Neutron Scattering. In: Molecular Motions in Liquids. Edited by J. Lascombe (D. Reidel Publishing Company, Dordrecht-Holland (1974) 641-467.
- C.T. Chang. Studies of Separation Distances in a Magnetically Driven Shock Tube with Parallel-Plate Electrodes. Z. Naturforsch. 29a (1974) 1838-1845.
- G.B. Christoffersen, V.O. Jensen, and P. Michelsen, Investigation of Ion Acoustic Waves in Collisionless Plasmas. Phys. Fluids 17 (1974) 390-399.
- E. Cohen, M.D. Sturge, R.J. Birgenau, E.I. Blount, L.G. Van Uitert, and J.K. Kjems, Internal Displacement Order Parameter below the 151 K Phase Transition in PrAlO<sub>3</sub>. Phys. Rev. Lett. 32 (1974) 232-235.

- N. D'Angelo, H.L. Pécseli, and P.I. Petersen, Comments on "Experimental Studies of Electrostatic Fluctuations in a Turbulently Heated Plasma". Phys. Fluids 17 (1974) 1789.
- N. D'Angelo, H.L. Pécseli, and P.I. Petersen, Turbulence in a Cusp Q-Device. Phys. Fluids 17 (1974) 1853-1856.
- N. D'Angelo, H.L. Pécseli, and P.I. Petersen, The Farley Instability: A Laboratory Test. J. Geophys. Res. 79 (1974) 4747-4751.
- O. Danielsen, Quantum Mechanical Operator Equivalents and Magnetic Anisotropy of the Heavy Rare Earth Metals. Risø Report No. 295, (1973) 227 pp.
- O.W. Dietrich, R.A. Cowley, and S.M. Shapiro, The Structure of Ferroelastic DCsDA, J. Phys. C 7 (1974) L239-L242.
- O.W. Dietrich and H.J.M. Hansen, Frygten for det ukendte. Alborg Stiftstidendes kronik ("Fear of the Unknown", newspaper article) (8 April 1974).
- A. Furrer and E. Warming, Crystal-field Splittings of NdS and NdSe, J. Phys. C 7 (1974) 3365-3368.
- E.H. Graf, V.J. Minkiewicz, H. Bjerrum Møller, and L. Passell, A Neutron Scattering Study of Collective Excitations in Superfluid Helium. Phys. Rev. A 10 (1974) 1748-1761.
- B. Hurup Hansen, A New Method for Calibrating the Time Delay of a Piezoelectric Probe. J. of Phys. F 7 (1974) 790-791.
- H. Heer, A. Furrer, E. Walker, A. Treyvand, H.-G. Purwins, and J. Kjems, Neutron Crystal-field Spectroscopy and Susceptibility in  $\text{Er}_{1-c}\text{Y}_c\text{Al}_2$ . J. Phys. C 7 (1974) 1207-1213.
- I. Heilman, J.M. Knudsen, N.B. Olsen, B. Buras, and J. Ståun Olsen, Studies of Thermal Decomposition of  $(\text{NH}_4)_2\text{Fe}(\text{SO}_4)_2 \cdot 6\text{H}_2\text{O}$ . Solid State Commun. 15 (1974) 1481-1484.
- J.G. Houmann, P. Bak, H.-G. Purwins, and E. Walker, Dispersion Relations for Magnetic Excitons in  $\text{NdAl}_2$ . J. Phys. C 7 (1974) 2691-2696.



- G. Jensen, L. Kristensen, and J. Taagholt, Unmanned Geophysical Observations in North Greenland 1972-1974. Danish Meteorological Institute, Copenhagen (1974) 77 pp.
- J. Jensen, Anisotropic Exchange Interaction in the Conical Magnetic Phase of Erbium. J. Phys. F 4 (1974) 1065-1072.
- N.O. Jensen, Vindkraft ("Wind Power"). Ingeniør og Bygningsvæsen 69 No. 17 (26 April 1974) 17.
- V O. Jensen, P. Michelsen, and H.C.S. Hsuan. Absolute and Convective Ion Beam Instability Studied through Green's Function. Phys. Fluids 17 (1974) December.
- V.O. Jensen, Status fra Fusionsforskningen. ("The Present Stage of Fusion Research"). Ingeniørens Ugeblad No. 40, (4 October 1974) 24.
- J.K. Kjems, L. Passell, H. Taub, and J.G. Dash, Neutron Scattering from Nitrogen Adsorbed on Basal-plane Oriented Graphite. Phys. Rev. Lett. 32 (1974) 724-727.
- L. Kristensen, Some Aspects of the Application of Digital Technique on Stochastic Time Series. Risø-M-Report No. 1766 (1974) 36 pp.
- S.E. Larsen and E.L. Petersen, Statistical Description of Air Pollution Concentration, Averaging Time and Frequency. Summary. Proceedings of the 5th Meeting of the Expert Panel on Air-Pollution Modeling, Risø, 1974. (NATO/CCMS, Bruxelles, 1974). 30.1-30.5.
- S.E. Larsen and E.L. Petersen, Statistical Description of Air Pollution Concentration, Averaging Time and Frequency. Symposium on Atmospheric Diffusion and Air Pollution, Santa Barbara, 1974. (AMS, Boston, 1974), 163-168.

- S.E. Larsen and N.E. Busch, Hot-Wire Measurements in the Atmosphere. Part I: Calibration and Response Characteristics. DISA Inf. 16 (1974) 15-34.
- B. Lebech and B.D. Rainford, Applied Magnetic Field Effects in Double-Hexagonal-Close-Packed Neodymium. Proceedings of the International Conference on Magnetism, 3 (1973) 191-195.
- B. Lebech, B.D. Rainford, and F.A. Wedgwood, The Magnetic Form Factor of Praseodymium Metal. Proceedings of the International Conference on Magnetism, Moscow, 2 (1973) 248-249.
- P.-A. Lindgård, Tables of Products of Tensor Operators and Stevens Operators, Risø Report, No. 313 (1974) 180 pp.
- P.-A. Lindgård and S.H. Liu, Exchange Interaction in the Heavy-Rare Earth Metals Calculated from Energy Bands. Proceedings of the International Conference on Magnetism, Moscow, 4 (1973) 40.
- P.-A. Lindgård, Exchange Interaction in the Heavy Rare Earth Metals Calculated from Energy Bands. Risø-M-Report No. 1701 (1974) 17 pp.
- P.-A. Lindgård and O. Danielsen, Theory of Magnetic Properties of Heavy Rare Earth Metals: Temperature Dependence of Magnetization, Anisotropy, and Resonance Energy. Phys. Rev. B 11 (1974) 351-362.
- P.-A. Lindgård and O. Danielsen, Bose-Operator Expansions of Tensor Operators in the Theory of Magnetism. J. Phys. C 7 (1974) 1523-1535.
- P. Michelsen and J.L. Hirsfield, Non-linear Excitation of Ion Acoustic Waves. Phys. Fluids 17 (1974) December.

- H.L. Pécseli, A Pedestrian Approach to Thermal Fluctuations and Noise. Seminar notes. Risø-M-Report No. 1710 (1974) 83 pp.
- H.L. Pécseli, Teoretisk beskrivelse af perturbationers udbredelse i et plasma. ("A Theoretical Description of Perturbation Propagation in a Plasma"). Risø-M-Report No. 1733 (1974) 65 pp.
- H.L. Pécseli, Investigations of Plasma Dielectric Functions. Risø Report No. 301 (1974) 28 pp.
- H.L. Pécseli, Linear Plasma Oscillations Described by a Superposition of Normal Modes. Phys. Fluids 17, (1974) 378-383.
- P.I. Petersen, Experimental Investigation of Plasmas in a Q-Machine. Risø-M-Report No. 1739 (1974) 63 pp.
- H.-G. Purwins, J.G. Houmann, P. Bak, and E. Walker, Interaction between Magnons and Magnetic Excitons in  $TbAl_2$ . Phys. Rev. Lett. 31 (1973) 1585-1587.
- H.-G. Purwins, E. Walker, B. Barbara, M.F. Rossignol, and P. Bak, Magnetization, Magnetocrystalline Anisotropy and the Crystalline Electric Field in Rare-Earth  $Al_2$  Compounds, J. Phys. C 7 (1974) 3573-3581.
- O. Rathmann, J. Als-Nielsen, P. Bak, J. Høg, and P. Touborg, Crystal Fields in  $Er_{0.02}Y_{0.98}$ . Phys. Rev. B 10 (1974) 3983-3987.
- O. Rathmann and J. Als-Nielsen, Long-range Order in  $\beta$ -brass Studied by Neutron Diffraction. Phys. Rev. B 9, (1974) 3921-3926.
- P.A. Reynolds, J.K. Kjems, and J.W. White, Lattice Vibrations in Chlorobenzenes: Experimental Dispersion Curves for  $\beta$ -para-dichlorobenzene by Neutron Scattering. J. Chem. Phys. 60 (1974) 824-834.

G. Shirane and J. Als-Nielsen, Formfactor in Fe at Small Wave Vectors by Magnetic Inelastic Scattering of Neutrons. Proceedings of the International Conference on Magnetism, Moscow, 2 (1973) 255-259.

Flemming Øster, The Reactor Refuelling Problem and the Possibility of a Pellet Injection Solution. In: The Present State of Research into Plasma Heating and Injection Methods. EUR FU 74/AGHI 10/R1 (Euratom, 1974) 103-106.

### Conference Contributions

J. Als-Nielsen and L.M. Holmes,  $\text{LiTbF}_4$  - A Model System of the Dipolar Ising Ferromagnet. Danish Society for the Physics and Chemistry of Condensed Matter. General Meeting, Helsingør, 23-25 May 1974.

P. Bak and J.G. Houmann, Magnetic Excitations in  $\text{NdAl}_2$ . Danish Society for the Physics and Chemistry of Condensed matter. General Meeting, Helsingør, 23-25 May 1974.

P. Bak, Magnetic Excitations in Rare Earth  $\text{Al}_2$  Compounds. 20th Annual Conference on Magnetism and Magnetic Materials, San Francisco, California, 3-6 December 1974.

M.M. Beg, Frequency Distribution of  $\beta$ -PdH at  $150^\circ\text{C}$  and  $200^\circ\text{C}$  using Cold Neutrons. Danish Society for the Physics and Chemistry of Condensed Matter. General Meeting, Helsingør, 23-25 May 1974.

H. Bjerrum Møller and T. Riste, Neutron Scattering Study of Orientational Order and Fluctuations at the Nematic-Isotropic Transition of Para-Azoxyanisole (PAA). 5th International Liquid Crystal Conference, Stockholm, Sweden, 17-21 June 1974.

B. Buras, B. Lebech, W. Kofoed, and G. Bäckström, Neutron Diffraction Studies under High Pressure. 17th Annual Meeting of the European High-Pressure-Research Group, Marburg, Germany, 19-21 March 1974.

- N.E. Busch, A Simple, Time-Dependent Model of the Planetary Boundary-Layer. European Mechanics Colloquim 51, The University of Cambridge, England, June 1974.
- N.E. Busch, Boundary-Layer Meteorology. 2nd Annual Meeting of the Danish Physical Society, Aarhus, 8-9 November 1974.
- K. Carneiro, Neutron Experiments on Solid and Liquid Hydrogen. International Summer School on Quantum Solids and Liquids, Kimberley, Ontario, Canada, 18-31 August 1974.
- C.T. Chang, On the Magnetic Shielding Effect of a Refuelling Pellet. Symposium on Plasma Heating in Toroidal Devices, Varenna, Lago di Como, Italy, 3-17 September 1974.
- O.W. Dietrich, R.A. Cowley, and S.M. Shapiro, The Spiral Structure of Ferroelectric DCsDA. Danish Society for the Physics and Chemistry of Condensed Matter. General Meeting, Helsingør, 23-25 May 1974.
- P.Aa. Hansen, The Magnetic Formfactor of  $\text{Pr}_{0.75}\text{Nd}_{0.25}$  Studied by Elastic Neutron Scattering. Danish Society for the Physics and Chemistry of Condensed Matter, General Meeting, Helsingør, 23-25 May 1974.
- B.N. Harmon, P.-A. Lindgård, A.J. Freeman, and J. Rath, Theoretical Magnon Dispersion Curves for Gd. 20th Annual Conference on Magnetism and Magnetic Materials, San Francisco, California, 3-6 December 1974.
- J.G. Houmann, A.R. Mackintosh, B.D. Rainford, O.D. McMasters, and K.A. Gschneidner Jr., Magnetic Excitons in Prasedymium. 20th Annual Conference on Magnetism and Magnetic Materials, San Francisco, California, 3-6 December 1974.
- J. Jensen, Anisotropic Exchange Interaction in the Conical Magnetic Phase of Erbium. Danish Society for the Physics and Chemistry of Condensed Matter. General Meeting, Helsingør, 23-25 May 1974.

- V.O. Jensen and P. Michelsen, Absolute and Convective Ion Beam Instability, Studied through Green's Functions. Plasma- og Gassutladningssymposiet, Geilo, Norway, 6-9 February 1974.
- V.O. Jensen, Status of Fusion Research, 2nd Annual Meeting of the Danish Physical Society, Aarhus, 8-9 November 1974.
- O. Jepsen, Electronic Energy Bands and Density of States of hcp Li, Na, K, Be, Yb, and sc  $\text{Pd}_3\text{Fe}$ . Band Structure Meeting, Göteborg, Sweden, 28-30 March 1974.
- L.W. Jørgensen, Massetab for Brintpiller i brint- og helium-plasmaer. ("Mass Loss of Hydrogen Pellets in Hydrogen and Helium Plasmas"). Plasma- og Gassutladningssymposiet, Geilo, Norway, 6-9 February 1974.
- J.K. Kjems, R.J. Birgeneau, G. Shirane and L.G. Van Uitert, Dynamics of the Cooperative Jahn-Teller Transition in  $\text{PrAlO}_3$ . Gordon Conference on Quantum Solids and Fluids, New Hampshire, August 1974. (Work performed under the auspices of the USAEC).
- J.K. Kjems, L. Passell, H. Taub, and G. Dash, Nitrogen Adsorbed on Graphite Studied by Neutron Scattering. American Physical Society, March Meeting, Philadelphia, Pennsylvania, March 1974. (Work performed under the auspices of the USAEC).
- J.K. Kjems, L. Passell, H. Taub, and G. Dash, Nitrogen Adsorbed on Graphite Studied by Neutron Scattering. Nordita Conference on Solid Surfaces, Niels Bohr Institute, Copenhagen, November 1974. (Work performed under the auspices of the USAEC).
- L. Kristensen, Automatisk indsamling af klimatologiske data i Nord-Grønland ("Automatic Collection of Climatological Data in North Greenland"). 9th Nordic Meeting on Meteorology, Bergen, Norway, 4-7 June 1974.

- S.E. Larsen and E.L. Petersen, Statistical Description of Air Pollution, Averaging Time and Frequency. 5th Meeting of the Expert Panel on Air Pollution Modeling, Risø, 4-6 June 1974.
- P.-A. Lindgård, Exchange Interaction in the Heavy Rare Earth Metals Calculated from Energy Bands, 11th Annual Winter School in Theoretical Physics, Karpacz, Poland, 18 February - 2 March 1974.
- P.-A. Lindgård and O. Danielsen. Theory of Magnetic Properties of Heavy Rare Earth Metals: Temperature Dependence of Magnetization, Anisotropy and Resonance Energy. 11th Annual Winter School in Theoretical Physics, Karpacz, Poland 18 February-2 March 1974.
- P.-A. Lindgård, Crystal Field Theory Including Fluctuations of the Molecular Field. Danish Society for the Physics and Chemistry of Condensed Matter. General Meeting, Helsingør, 23-25 May 1974.
- M. Nielsen, Neutron Scattering in Solid Para-Hydrogen. Conference on Quantum Crystals, Tbilisi, U.S.S.R., 11-15 November 1974.
- H.L. Pécseli, Experimental Investigation of the Farley Instability in a Single-ended Q-Machine. Plasma og Gassutladningssymposiet, Geilo, Norge, 6-9 February 1974.
- E.L. Petersen, Statistical Description of Air Pollution Concentration, Averaging Time and Frequency. Symposium on Atmospheric Diffusion and Air Pollution, Santa Barbara, California 9-13 September 1974.
- P.I. Petersen, Turbulence in a Cusp Q-Device. Plasma og Gassutladningssymposiet, Geilo, Norge, 6-9 February 1974.
- B.M. Powell, Neutron Scattering Studies of Molecular Vibrations. Danish Society for the Physics and Chemistry of Condensed Matter. General Meeting, Helsingør, 23-25 May 1974.

- T. Riste and H. Bjerrum Møller, Critical Neutron Scattering of the Nematic-Isotropic Transition of PAA. Gordon Research Conference on Liquid Crystals, Santa Barbara, California, 14-18 January 1974.
- O. Rathman, J. Als-Nielsen, and P. Bak, Crystal Fields in  $\text{Er}_{0.02}\text{Y}_{0.98}$  Studied by Neutron Scattering. Danish Society for the Physics and Chemistry of Condensed Matter. General Meeting, Helsingør, 23-25 May 1974.
- O. Rathman, J. Als-Nielsen, and P. Bak, Crystal Fields in  $\text{Er}_{0.02}\text{Y}_{0.98}$  Studied by Neutron Scattering. Conference on Crystalline Electrical Field, Montreal, Canada, 26-29 June 1974.
- S.M. Shapiro, O.W. Dietrich, G. Shirane, and J.P. Axe, Measurements of Electron Phonon Interaction in Superconductors by Inelastic Neutron Scattering. Danish Society for the Physics and Chemistry of Condensed Matter. General Meeting, Helsingør, 23-25 May 1974.
- H. Sørensen, Backscattered Energy from Light-Ion-Bombarded Gold by a Low-Temperature Calometric Method. Symposium on Multiple Scattering of Ions and Related Energy Loss Problems, H.C. Ørsted Institute, Copenhagen, 10 December 1974.

Degrees, Students, etc.

During the period the following members of the staff acquired the following degrees:

Per Bak	lic. techn.
Kim Carneiro	lic. techn.
Oluf Danielsen	lic. techn.
Hans Pécseli	lic. techn.
Peter I. Petersen	lic. scient.
Niels Woetmann Nielsen	cand. scient.



The following postgraduate students carried out research at the Physics Department leading to the degrees of lic. techn. and lic. scient.:

Peter Aarosiin Hansen	(Solid State Physics)
Niels Otto Jensen	(Meteorology)
Leif Wagner Jørgensen	(Plasma Physics)
Ole Rathmann	(Solid State Physics)
Jack Wenzel (Ph.D.)	(Solid State Physics)

The following students from Danish universities are working on M.Sc. thesis projects at the department:

Jens Juul Rasmussen	(Plasma Physics)
Klaus Hedegaard	(Meteorology)

During January and August 1974 students from the Universities of Århus and Copenhagen took part in laboratory courses organized by staff members. The following courses were offered:

- 1) Neutron Scattering (K. Carneiro, W.D. Ellenson and E. Warming).
- 2) Plasma Physics (P. Michelsen, H.L. Pécseli and P.I. Petersen).

Two foreign students sponsored by the IAESTE carried out practical work at the department as part of their general training.

7. STAFF OF THE PHYSICS DEPARTMENT

Hans Bjerrum Møller (head of the department)

Office Staff

Jonna Christensen (until September 30)

Alis Frellsen (until June 30)

Gerda Stauning

Grethe Sørensen

Alice Thomsen

Anne-Lise Katholm (temporary assistant)

1. Solid-State Physics (Neutron Physics)

Scientific Staff

Jens Als-Nielsen

Ole Krogh Andersen (consultant from Technical University of Denmark)

Mansoor M. Beg (guest scientist from Pakistan Institute of Nuclear Science and Technology)

Per Bak (lic. techn. student) (until August 10)

Bronislaw Buras (guest scientist from H.C. Ørsted Institute)

Kim Carneiro (lic. techn. student) (until August 15)

Maurice Chapellier (consultant from H.C. Ørsted Institute) (until September 26)

Rodney M.J. Cotterill (consultant from Technical University of Denmark)

Ove W. Dietrich

William D. Ellenson (guest scientist from University of California)

Peter Aarosiin Hansen (lic. techn. student)

Jens Gylden Houmann

Jens Jensen (until October 31)

Ove Jepsen

Jørgen Kjems

Jens Klæstrup Kristensen (lic. techn. student from the  
Technical University of Denmark)

Bente Lebech

Per-Anker Lindgård

Hans Bjerrum Møller

Mourits Nielsen

Ole Rathmann (lic. techn. student)

Stephen M. Shapiro (guest scientist from Brookhaven  
National Laboratory) (until September 6)

Elisabeth Warming

Jack Wenzel (Ph.D. student from the University  
of Chicago) (until April 30)

Technical Staff

Bjarne Breiting

Kaj Christensen

Arent Hansen

Bent Heiden

John Z. Jensen

Louis G. Jensen

Steen Jørgensen

Werner Kofoed

Jens Linderholm

Jørgen Munck

Allan Thuesen

Knud Møllenbach (temporary assistant)

## 2. Plasma Physics

### Scientific Staff

Che Tyan Chang

Nicola D'Angelo (consultant from Danish Space Research Institute)

Vagn O. Jensen

Leif Wagner Jørgensen (lic. techn. student)

Poul Michelsen

Hans Pécseli

Peter I. Petersen (until September 13)

Alfred H. Sillesen

Hans Sørensen

Chan Mou Tchen (consultant from City University of New York)

Flemming Øster

### Technical Staff

Bengt Hurup Hansen

Mogens Nielsen

Arne Nordskov

John Petersen

Børge Reher

Hans Skovgård

Jane Doyle Lynggård (temporary assistant)

## 3. Nuclear Physics

### Scientific Staff

Verner Andersen

Carl Jørgen Christensen

### Technical Staff

Poul Andersen

Finn Hansen

#### 4. Meteorology

##### Scientific Staff

Niels E. Busch

Ole Christensen (from ISVA, The Technical University of Denmark)

Niels Otto Jensen (lic. techn. student)

Leif Kristensen

Søren E. Larsen

Niels Woetmann Nielsen (temporary assistant)

Erik Lundtang Petersen

Chan Mou Tchen (consultant from City University of New York)

##### Technical Staff

Jørgen Christensen

Gunner Dalsgaard

Morten Frederiksen

Gunnar Jensen

Knud Sørensen

#### 5. Liquid N<sub>2</sub> and He Plant

##### Technical Staff

John Z. Jensen

Poul E. Bredahl (Until April 30)

Bent Ferdinansen (part time assistant from the Service Department)

8. VISITING SCIENTISTS  
(one to three months' visits)

A. Blackadar Pennsylvania State University	(Meteorology)
N.E.J. Boston Naval Postgraduate School, Monterey	(Meteorology)
F.H. Champagne University of California, San Diego	(Meteorology)
T. Deaton University of California, San Diego	(Meteorology)
D. Dimock Princeton University	(Plasma Physics)
C.A. Friehe University of California, San Diego	(Meteorology)
C.H. Gibson University of California, San Diego	(Meteorology)
T. Giebułtowiec Institute of Experimental Physics, Warsaw	(Solid-State Physics)
T.M. Houlihan Naval Postgraduate School, Monterey	(Meteorology)
F.E. Jerome Malispina College, British Columbia	(Meteorology)
J. laRue University of California, San Diego	(Meteorology)
G.A. Mackenzie University of Edinburgh	(Solid-State Physics)
C.A. Paulson Oregon State University	(Meteorology)
G.S. Pawley University of Edinburgh	(Solid-State Physics)
G. Pepy Centre d'Études Nucléaires de Saclay, Gif-sur-Yvette	(Solid-State Physics)
E.W. Peterson Oregon State University	(Meteorology)
D. Pettifor Imperial College, London	(Solid-State Physics)

M. Platiša Institute of Physics, Beograd	(Plasma Physics)
M. Popović Institute of Physics, Beograd	(Plasma Physics)
B.M. Powell Chalk River, Canada	(Solid-State Physics)
B.D. Rainford Imperial College, London	(Solid-State Physics)
T. Riste IFA, Kjeller	(Solid-State Physics)
R.M. Williams Oregon State University	(Meteorology)

